Effects of constitutive and acute Connexin 36 deficiency on brain-wide susceptibility to PTZ-induced neuronal hyperactivity

Alyssa A. Brunal-Brown

Dissertation submitted to the Faculty Virginia Polytechnic Institute and State University in partial fulfillment of the requirements of the Degree of

Doctor of Philosophy

In

Translational Biology, Medicine, and Health

Y. Albert Pan, Ph.D., Chair

James W. Smyth, Ph.D.

Susan Campbell, Ph.D.

Michelle Olsen, Ph.D.

September 2020

Roanoke, VA

Keywords: Connexin 36 (Cx36), epilepsy, seizures, whole-brain activity, whole-brain expression

Effects of constitutive and acute Connexin 36 deficiency on brain-wide susceptibility to PTZ-induced neuronal hyperactivity

Alyssa A. Brunal-Brown

ABSTRACT

Connexins are transmembrane proteins that form hemichannels allowing the exchange of molecules between the extracellular space and the cell interior. Two hemichannels from adjacent cells dock and form a continuous gap junction pore, thereby permitting direct intercellular communication. Connexin 36 (Cx36), expressed primarily in neurons, is involved in the synchronous activity of neurons and may play a role in aberrant synchronous firing, as seen in seizures. To understand the reciprocal interactions between Cx36 and seizure-like neural activity, we examined three questions: a) does Cx36 deficiency affect seizure susceptibility, b) does seizure-like activity affect Cx36 expression patterns, and c) does acute blockade of Cx36 conductance increase seizure susceptibility. We utilize the zebrafish pentylenetetrazol (PTZ; a GABA(A) receptor antagonist) induced seizure model, taking advantage of the compact size and optical translucency of the larval zebrafish brain to assess how PTZ affects brain-wide neuronal activity and Cx36 protein expression. We exposed wild-type and genetic Cx36-deficient (cx35.5-/-) zebrafish larvae to PTZ and subsequently mapped neuronal activity across the whole brain, using phosphorylated extracellular-signal-regulated kinase (pERK) as a proxy for neuronal activity. We found that cx35.5-/- fish exhibited region-specific susceptibility and resistance to PTZ-induced hyperactivity compared to wild-type controls, suggesting that genetic Cx36 deficiency may affect seizure susceptibility in a region-specific manner. Regions that showed increased PTZ sensitivity include the dorsal telencephalon, which is implicated in human epilepsy, and the lateral hypothalamus, which has been underexplored. We also found that PTZ-induced

neuronal hyperactivity resulted in a rapid reduction of Cx36 protein levels within. 30 minutes and one-hour exposure to 20 mM PTZ significantly reduced the expression of Cx36. This Cx36 reduction persists after one-hour of recovery but recovered after 3-6 hours. This acute downregulation of Cx36 by PTZ is likely maladaptive, as acute pharmacological blockade of Cx36 by mefloquine results in increased susceptibility to PTZ-induced neuronal hyperactivity. Together, these results demonstrate a reciprocal relationship between Cx36 and seizure-associated neuronal hyperactivity: Cx36 deficiency contributes region-specific susceptibility to neuronal hyperactivity, while neuronal hyperactivity-induced downregulation of Cx36 may increase the risk of future epileptic events.

Effects of constitutive and acute Connexin 36 deficiency on brain-wide susceptibility to PTZ-induced neuronal hyperactivity

Alyssa A. Brunal-Brown

GENERAL AUDIENCE ABSTRACT

Within the brain, cells (neurons) communicate with each other to pass along information. This communication is important for normal functions of the brain such as learning and memory, muscle movement, etc. Epilepsy is a disease of the brain that is caused by rapid over synchronized communication between cells. This leads to seizures which can include convulsions, loss of attention, and much more. Currently, 30% of patients suffering from epilepsy do not have a treatment option that works for them, it is, therefore, imperative to investigate new targets for treatment in this disease. Connexin36 is a protein in the brain that directly connects cells so they can pass information quickly between them. Connexin36, therefore, might make a good target for treatment. Previous work has aimed to understand this relationship but has been limited in their ability to look at the entire brain at any one time. The goal of this study was to understand the relationship between connexin 36 and brain hyperactivity across the whole brain simultaneously. To understand this relationship, we first determined what happened to brain activity if the protein was missing entirely after exposure to a seizure causing drug. We were asking: How does connexin 36 affect hyperactivity. We found that different regions of the brain responded differently without the connexin 36 protein. This suggests that one size does not fit all, and one must look at the whole brain to understand the effects of the connexin 36 protein. Next, we asked a similar question, but in the opposite direction, how does hyperactivity affect connexin 36? We found, in the short-term, hyperactivity reduced the amount of connexin 36 present in certain regions of the brain. This continued until 3 hours following exposure to the seizure causing drug Pentylenetetrazol (PTZ).

Lastly, to determine if this short-term reduction in connexin 36 meant that an individual was more likely to experience hyperactivity. To do this, we used a connexin 36 blocking drug, then introduced the seizure causing drug at different concentrations. We found, at all concentrations, the connexin 36 blocking drug caused significant changes in neuronal activity, depending on the brain regions. Overall, our results showed that connexin 36 plays an important role in hyperactivity and that a short-term reduction in connexin 36 is detrimental, and may contribute to an increase in the possibility of subsequent hyperactivity.

Acknowledgments

I would like to thank my advisor, Dr. Albert Pan for his mentorship and guidance throughout my graduate training. He has fostered my development and independence as a scientist and these skills will continue to serve me throughout my career.

I would like to express my gratitude to my dissertation committee, Dr. James Smyth, Dr. Susan Campbell, and Dr. Michelle Olsen for their valuable guidance and feedback throughout my project.

I would like to give special thanks to both current and former members of the Pan lab, Dr. Kristin Ates, Dr. Manxiu Ma, and Dr. Kareem Clark. Each of them taught me everything I know about zebrafish and molecular biology techniques. I also want to thank them for all the fun times we had both inside and outside the lab, and the lasting friendships I've made.

Lastly, I would like to thank my family for their unwavering support. I would like to thank my parents and siblings for always believing in me and supporting me to do whatever I put my mind to. Thank you to my wonderful loving husband who has been my rock through the graduate school process. I wouldn't be here without their support**.**

Table of Contents

List of Figures

List of Abbreviations

Cx36, Connexin 36

Cx43, Connexin 43

PTZ, pentylenetetrazol

BBB, Blood-brain barrier

tERK, total extracellular signal-regulated kinase

pERK, phosphorylated extracellular-signal-regulated kinase

MAP-mapping- Mitogen-Activated Protein Kinase- mapping

CMTK, Computational Morphometry Toolkit

dpf, days post-fertilization

PFA, paraformaldehyde

TCA, trichloroacetic acid

DMSO, dimethyl sulfoxide

GABA, Gamma aminobutyric acid

CAMKII, Ca2+/calmodulin-dependent protein kinase II

PKA, Protein Kinase A

PKC, Protein Kinase C

cx35.5-/-, Connexin 35.5 deficient fish

Ca^{2+}, Calcium

JME, Juvenile Myoclonic Epilepsy

NAv1.1, Type I voltage-gated sodium channel

LTP, Long-term potentiation

LTD, Long-term depression

EEG, Electroencephalogram

K^{+}, Potassium

ALS, Amyotrophic lateral sclerosis

4-AP, 4-Aminopyridine

ER, Endoplasmic Reticulum

TGN, Trans-Golgi Network

cdc2, cyclin-dependent kinase

TLE, Temporal Lobe Epilepsy

CHAPTER 1: INTRODUCTION

1.1 The Cellular Components of the Brain

The brain is the organ responsible for collecting and interpreting information about the world around us. With integrated information, it performs calculations and coordinates an organism's actions to ensure its survival. The brain is made up of many cell types, each serving its function in this retrieval, processing, and output function. These cell types are split into two main groups: neurons and glia.

Neurons are the main computational unit of the brain, performing most computational processes. These cells communicate through both electrical and chemical signals and directly transfer information from one cell to the next. Neurons fall into two main groups based on functionality: excitatory, inhibitory, and modulatory neurons (Squire et al. 2012). Excitatory neurons are responsible for passing along information and propagating signals. Inhibitory neurons are responsible for preventing signal propagation. Each of these types of neurons plays an important role in the computational process in the brain. Excitatory neurons utilize the neurotransmitter glutamate. Glutamate causes an influx of ions into the cell, leading to depolarization. If a cell receives enough excitatory input, that cell reaches the depolarization threshold and an action potential is initiated. Inhibitory neurons on the other hand utilize the neurotransmitter Gamma-Aminobutyric acid (GABA). This causes a hyperpolarization of the cell, pulling it farther away from reaching threshold, making it less likely to fire. Each neuron receives excitatory and inhibitory inputs but depending on the ratio of each of these inputs, determines if that cell fires or not (Squire et al. 2012).

Glia are a diverse group of support cells responsible for the many processes integral to the overall function of the brain. The different glial cell types include astrocytes, microglia, and oligodendrocytes. The most abundant glial cell in the brain is astrocytes. They serve to maintain the blood-brain barrier, manage ion homeostasis, support synapses, neuron guidance, and response to injury. Microglia are the innate immune cells of the brain. They serve major roles in the prevention of infection by pathogens, removal of debris and waste, and pruning of synapses. Oligodendrocytes are cells that encapsulate the axons of neurons and create insulation to speed up neuronal communication (Squire et al. 2012).

1.2 The basis of neuronal communication: chemical and electrical synapses

The cellular structure of neurons is essential for their communication with other cells in the brain. A typical neuron has four main cellular compartments: the dendrite, soma, axon, and nerve terminal. An action potential (electrical signal) travels down that cell's axon and reaches the nerve terminal where it triggers a release of intracellular calcium, which triggers the release of neurotransmitters into the synaptic cleft. Those neurotransmitters then travel across the synapse and bind to receptors on the next cell and trigger an action potential in the next cell. This action potential then travels down the cell's dendrite, through the soma, down the axon, and then the process repeats.

Neurons require a specific level of depolarization to reach the threshold for an action potential (which is an all or nothing response). Each neuron receives thousands of inputs and has thousands of outputs. Each of those inputs may serve a different function related to the inputting cell type mentioned previously. Excitatory neurons function to relay information, they send information and use neurotransmitters (ie. glutamate, dopamine) that propagate that signal further through some magnitude of depolarization of the next cell. Inhibitory neurons, on the other hand,

act oppositely, they reduce the propagation of the signal through hyperpolarization of the cell or by inhibiting another inhibitory neuron. With each cell receiving thousands of inputs, there is a summation of all these inputs which determines if a cell reaches threshold for an action potential (thus the signal is passed along). If there is an excess of inhibitory signals, and there is no action potential (and thus no signal). This is how the brain performs computations. There is a second type of communication between neurons, however, through an electrical synapse.

Electrical synapses function differently from chemical synapses in a few key ways. While an action potential is still propagated through a cell and reaches the nerve terminal, ions from the pre-synaptic cell can directly travel across the membrane into the post-synaptic cell through a pore called a gap junction. Gap junctions consist of proteins known as connexins. Connexin proteins are dynamically regulated and their transport and function can be altered by many factors. The protein is transcribed in the nucleus and the mRNA is transported to free ribosomes where is it is translated. The mRNA ribosome complex is then transported to the rough ER. The newly translated protein is then transported through the smooth ER. If the protein is properly folded, it is then transported to the Golgi, if the protein is not properly folded, it is poly-ubiquitinated and sent for degradation. Once in the Golgi, specifically the trans-Golgi network (TGN) the protein is oligomerized into a hexamer to create a connexon, a single hemichannel pore. The connexon is then transported in a vesicle along actin filaments with the assistance of microtubules to the cell surface where it is either implanted alone, forming a hemichannel, and allowing for cellular communication with the extracellular space or docks with an adjacent cell with another connexon. This process is directed with helper proteins such as ZO-1, ZO-2, and EB (Laird 2006). The two connexons from adjacent cells then dock together creating a pore connecting the cytoplasm of both cells which allows for the bidirectional flow of ions between cells (Laird 2006). Through this more

direct form of communication, neurons can communicate more quickly than through chemical synapses in both excitatory and inhibitory neurons (Purves et al. 2001). This also allows for synchronous firing of cells, which is important for various functions in the brain such as learning and memory (Haas, Zavala, and Landisman 2011; Wang and Belousov 2011), eye function (Mills et al. 2001; Telkes et al. 2019; Kovács-Öller et al. 2017), etc. This fast communication is also critically important for the development and maintenance of synapses and direct cell-to-cell communication.

Connexin gap junctions and connexon hemichannels are internalized and endocytosed via clathrin-mediated endocytosis. The entire gap junction complex (also known as the annular junction or connexosome) is endocytosed by one cell, and the protein is then transferred to a lysosome for degradation. Cytosolic stress can prevent the transfer of connexin proteins from endosomes to the lysosome. (Laird 2006). The endocytosis of connexons and gap junctions is regulated by phosphorylation of the C-terminus. Various kinases are involved in endocytosis of connexin proteins, such as mitogen-activated protein kinase (MAPK), protein kinase C (PKC), protein kinase A (PKA), cyclin-dependent kinase (cdc2), and casein kinase 1(Laird 2006). In addition to phosphorylation of the C-terminus, connexin hemichannels and gap junctions can be mono-ubiquitinated, which functionally serves as an internalization signal (Laird 2006).

1.3 Connexins: an avenue for neuronal communication in health and disease

Gap junction and hemichannel function allow for the fast and dynamic regulation of synchronous firing of cells across the body. As such, various aspects can affect either the function of the pore (through blockade or enhancement) or the presence of the pore through changes in implantation or degradation of the pore. Activity is a major regulator of gap junction proteins. In the heart, following ischemia, gap junction pores are blocked to protect the cells of the heart

(Schulz et al. 2015). In the brain, neuronal activity has been shown to either increase the functionality (allowing more current, LTP) of gap junction channels with high amounts of calcium(Wang and Belousov 2011), or decrease the functionality of gap junction channels with low amounts of calcium (allowing less current, LTD) (Haas, Zavala, and Landisman 2011). In astrocyte, regulation of Cx43 appears to be dependent on the activation state of the astrocyte. Pro-inflammatory cytokines, typically released by microglia, cause phosphorylation of Cx43, leading to internalization of the protein from the membrane thereby reducing overall membrane permeability of the cell (Retamal et al. 2007).

Throughout the body, there are many different types of connexin proteins. A subset of those are located within the brain. Two types of connexin proteins are most abundant within the brain: Connexin 43 (Cx43) and Connexin 36 (Cx36) and each serves a distinct function. Cx43 is located in many organs including the heart and brain (Harris and Locke 2008). In the brain, it is mostly located in astrocytes (Giaume and Naus 2013). In astrocytes, Cx43 acts as a direct pore between two cells, which allows for the free flow of ions like Ca^{2+} and K^{+} (Cotrina et al. 1998; Kofuji and Newman 2004). Through this interconnected network of astrocytes, ions can be shunted away from synapses and certain areas of the brain, which is important for the maintenance of homeostasis (Kofuji and Newman 2004). Dysfunction of this process may lead to malfunction of neuronal networks. Cx43 has been shown to play a very important role in the development of epilepsy. It has been shown that, after traumatic brain injury, astrocytes are less able to shunt ions away from the synapse, causing an increase in excitability of the synapse, which can lead to epilepsy (Shandra et al. 2019). In addition to the dispersion of ions, Cx43 acts as an important factor in maintaining the blood-brain barrier (BBB). Astrocytic endfeet wrap around the blood vessels of the brain creating a tight seal preventing most material from entering the brain. These end feet are rich in

connexin proteins and Cx43 and Cx30 specifically play an integral role in maintaining the BBB (Ezan et al. 2012).

Cx36 is found mostly on neurons and can be found on microglia (Giaume and Naus 2013). Cx36 is the primary connexin protein responsible for the synchronous firing of neurons within the brain (Rash et al. 2012). Cx36 plays an important role throughout development. Cx36 may affect neuronal migration and the development of synapses by physically maintaining contact between two cells before the development of chemical synapses (Belousov and Fontes 2013). In addition to functioning during development, Cx36 plays many roles within the mature brain as well. Cx36 may function in learning and memory through the strengthening and weakening of synapses through long-term potentiation and depression (LTP and LTD) (Wang and Belousov 2011; Haas, Zavala, and Landisman 2011). Additionally, electrical synapses can alter the rate of coupling between neurons, thereby offering independent control of neuron to neuron coupling (Smith and Pereda 2003). The role of Cx36 in disease isn't as well defined. Patients with Juvenile Myoclonic Epilepsy (JME) exhibit higher instances of a SNP in the non-coding region of Cx36 (Mas et al. 2004) which may affect protein folding, but this has not been confirmed (Hempelmann, Heils, and Sander 2006). SOD-1 deficient mice (a model for Amyotrophic lateral sclerosis (ALS)) and motorneuron samples from patients with ALS exhibit decreased Cx36, which may contribute to motor neuron dysfunction through enhancement of secondary cell death. That is to say that Cx36 functions to spread "death-signals" to other cells and leads to secondary cell death of motor neurons (Belousov et al. 2018). Finally, while Cx36 is most highly expressed in neurons, it is also expressed in microglia. Previous work has shown that activated microglia show decreased Cx36 expression, leading to decreases in the coupling between microglia and decreases in the coupling between microglia and neurons (Dobrenis et al. 2005).

As mentioned previously, connexin proteins are dynamically regulated and various aspects can change the functionality of the pore as well as removal and implantation in the membrane. In excitatory cells coupled with Cx36, phosphorylation of the Cx36 protein through the activation of the PKA pathway reduces pore functionality and reduces the likelihood of pore opening. While phosphorylation of the Cx36 protein through activation of the CAMKII protein leads to a decrease in expression therefore inhibiting the functionality of Cx36 (Bazzigaluppi et al. 2017). This discrepancy is likely due to differences in the phosphorylation site, demonstrating event-specific responses in gap junction plasticity (Bazzigaluppi et al. 2017). This is supported by recent work that has shown that both activity-dependent LTP (Wang and Belousov 2011) and LTD (Haas, Zavala, and Landisman 2011) of electrical synapses is calcium level-dependent, suggesting that either high or low levels of calcium may cause activation of different kinases and therefore phosphorylate at different sites on Cx36.

1.4 Diseases of communication: epilepsy

As mentioned previously, communication between neurons is the foundation of brain function. When there is a disruption in communication, the consequences can be devastating. The prime example of malfunctioning neuronal communication in disease are seizures. Seizures affect approximately 8-10% of the population within the U.S. (Annegers et al. 1995; Hauser, Annegers, and Kurland n.d.) and are characterized by events of rapid, uncontrolled synchronous firing within the brain which can lead to convulsions, loss of consciousness, memory loss, and even death (Krumholz et al. 1995). Prevention of seizures relies on a delicate balance of neuronal excitation and inhibition. Epilepsy is defined as two or more seizures within 24 hours.

There are two main categories of seizure: focal and generalized seizures. Focal seizures, which account for 60% of all seizures, affect one region of the brain like the temporal, frontal, or

occipital lobes (“Types of Seizures | Epilepsy | CDC” 2020; “Types of Epilepsy & Seizure Disorders in Adults | NYU Langone Health” 2020). The most common type of focal seizures affects the temporal lobe (Téllez-Zenteno and Hernández-Ronquillo 2012). Generalized seizures on the other hand involve more than just one area of the brain and increased electrical activity affects the entire brain. These typically present as absence seizures (loss of attention) or tonic-clonic seizures which present with whole-body convulsions (“Types of Seizures | Epilepsy | CDC” 2020; “Types of Epilepsy & Seizure Disorders in Adults | NYU Langone Health” 2020). Chronic seizures, presenting with two or more seizures per 24-hour period are identified as epilepsy (“Types of Epilepsy & Seizure Disorders in Adults | NYU Langone Health” n.d.). Approximately 1.2% of the U.S. population has some type of active epilepsy (Zack and Kobau 2017).

Some forms of epilepsy have a known genetic cause, such as Dravet syndrome. This is a disease affecting 1 in 15,700 births (Y. W. Wu et al., 2015) and is first observed within the first year of life as a convulsant seizure not caused by vaccination or fever. Seizures then become more chronic, in the majority of patients exhibiting myoclonic seizures. These seizures are severe and can lead to developmental delays, and they last into adulthood (Dravet 2011). A large portion of patients with the disease exhibit a genetic mutation in the type I voltage-gated sodium channel, Nav1.1 (Bender et al. 2012). This mutation results in a disruption of fast-spiking GABAergic neurons and results in altered excitation-inhibition balance. This can lead to seizures and some of the cognitive impairments observed in Dravet syndrome (Bender et al. 2012). Unlike Dravet syndrome, the causes of many more common seizures and epilepsies are unknown.

Current therapeutics are focused on managing symptoms and reducing seizures. They are separated into three distinct groups: those that increase the action of GABA, those that limit the action of glutamate, or those that focus on the functioning of voltage-gated ion channels (Davies

1995). Approximately 30% of those suffering from epilepsy don't respond to current antiepileptic drugs (Kwan and Brodie 2000). It is, therefore, imperative to identify novel targets for therapeutics that address these kinds of disorders.

1.5 Connexin proteins and seizures

Seizures are characterized by the rapid hypersynchronous firing of neurons. As such, connexin proteins and their function in synchronous firing of cells make connexins a prime target when examining potential therapeutic targets. Two main connexin proteins have been investigated for their involvement in seizures: Cx43 and Cx36. Cx43 is primarily expressed in astrocytes and plays an important role in ion homeostasis of the synapse. It functions to allow for the shunting of ions away from the synapse to prevent hyperexcitability (Shandra et al. 2019; Vincze et al. 2019). Additionally, previous studies examining the expression of different connexin proteins shows increases in the expression of Cx43 after seizure induction using multiple methods (Laura et al. 2015; Motaghi et al. 2017; Collignon et al. 2006; Garbelli et al. 2011).

Previous research regarding the role of Cx36 in seizures and epilepsy is conflicting. Changes in Cx36 expression following seizure induction are unclear, with some studies showing increased Cx36 expression after seizures (Laura et al. 2015; X. Wu et al. 2017), while others show a decrease (Condorelli et al. 2003; Söhl et al. 2000) or no change (Motaghi et al. 2017). Additionally, knock-out or inhibition of Cx36 using connexin blocking drugs produce mixed results (Gajda et al. 2005; Jacobson et al. 2010; Shin 2013; Voss, Mutsaerts, and Sleigh 2010a). A few limitations to these studies may explain their contradictory findings. For example, each study uses a different method of inducing seizures, which can make comparisons difficult. Additionally, due to limitations of the rodent model, each study is looking at limited brain regions, particularly the hippocampus. Finally, Cx36 is expressed in primarily inhibitory interneurons (Hestrin and

Galarreta 2005) but does show some expression in excitatory neurons (Vervaeke et al. 2010). Responses to hyperactivity with loss of Cx36 in these two subpopulations would be drastically different. Loss of Cx36 from inhibitory cells would lead to a dysfunction of the inhibitory circuit, therefore leading to an increased likelihood of hyperexcitation. On the other hand, loss of Cx36 in excitatory cells may lead to decreased excitation and hyperactivation. Regional differences in brain activity may be related to differences in cell-type expression of Cx36 and a cell-type specific response to hyperactivity.

1.6 The zebrafish as a model for epilepsy and seizures and connexin biology

To study epilepsy and seizures multiple methods and model organisms exist. Traditionally, rodent models and mouse models are most typically used. Using these animal models, different genetic and drug treatment options exist to model epilepsy and seizures. The most common chemical methods of inducing seizures in rodents include Kainic acid (kinate), Pentylenetetrazol (PTZ), 4-Aminopyridine (4-AP), and pilocarpine (Kandratavicius, Balista, et al. 2014).

Each of the drugs mentioned above has a different mechanism of action. Kainic acid acts as a chemical agonist increasing the activity of glutamate and excitatory cells and preferentially affects the hippocampus. Animals treated with Kainic acid typically develop spontaneous recurrent seizures and is therefore a good model of epilepsy and chronic disease (Kandratavicius, Balista, et al. 2014). PTZ acts on the opposite cell system. It acts as a GABA antagonist, preventing inhibition, leavening the animal with hyperactivation. PTZ does not cause chronic recurrent seizures, making it a better model for studying the acute effects of seizures (Kandratavicius, Balista, et al. 2014). Pilocarpine act as a muscarinic acetylcholine receptor agonist that leads to status epilepticus and inherent structural damage within the brain

(Kandratavicius, Alves Balista, et al. 2014a). This model is specific to studying status epilepticus and is not a good model for examining seizures or epilepsy.

In addition to drug-induced models of seizures and epilepsy, many labs utilize electrical initiation of seizures. Seizures can be induced using electroshock therapy involving a one time shock of 6 Hz in mice and 50-60 Hz in rats. This leads to myoclonic seizures. Repeated treatment (kindling) can lead to spontaneous recurrent seizures, making the kindling method a good model for epilepsy (Kandratavicius, Alves Balista, et al. 2014a).

A newer animal model of seizures and epilepsy uses the zebrafish. Zebrafish develop quickly and the small size of zebrafish larvae facilitates imaging of the whole brain under a laser scanning confocal microscope. After breeding, eggs are laid, and larvae develop over days (experiments can be performed as soon as 3 days post-fertilization). Genetic tools are widely available for zebrafish and are fast and easy to use. This allows for mutations, and transgenes to be introduced into the genome. As such, zebrafish are ideal for examining whole-brain activity and protein localization following seizure induction.

A common method of inducing hyperactivity in zebrafish uses PTZ, a GABA antagonist, in the water of zebrafish larvae (Baraban et al. 2005). Other methods of inducing hyperactivity found in rodent models, such as Kainic Acid, a glutamate agonist, can also be used (Kandratavicius, Balista, et al. 2014). Hyperactivity can be examined both in the brain and through behavior in a similar way to other models, through EEG (Cho et al. 2017), live calcium imagining (Diaz Verdugo et al. 2019; Liu and Baraban 2019), and behavior (Baraban et al. 2005). Additionally, newer technologies, such as the whole-brain activity mapping technique (MAP-map) developed by Randlett et al., 2015, offer a whole-brain resolution of brain activity and allows for the discovery of novel regions of interest.

In recent years, the zebrafish has been shown to act as an appropriate model of seizures and epilepsy, particularly in drug-screens. Baraban et al., 2005 first validated the zebrafish PTZ model for use in studying seizures. They treated larval zebrafish with varying concentrations of PTZ and observed their locomotor behavior. They categorized locomotor behavior into three categories: Stage I where fish dramatically increased their locomotor activity, Stage II where fish exhibited rapid "whirlpool-like" swimming patterns and convulsions, and finally Stage II where fish exhibited clonus-like convulsions followed by a loss of body posture. This was then validated using EEG, where they were able to identify specific ictal and inter-ictal events that were successfully modulated using synaptic transmission interfering drugs (Baraban et al. 2005). This work was then expanded by Baraban et. al., 2013 who developed a genetic mutant that modeled Dravet syndrome. They performed a high-throughput drug screen to examine which drugs caused a decrease in locomotor behavior. The antiepileptic properties of the identified drugs were then confirmed using EEG. Using this model, they were able to identify a novel compound, clemizole, that may treat this disease. Following this study, clemizole is now being tested in a clinical trial (Baraban, Dinday, and Hortopan 2013).

Approximately 70% of the genome of the Zebrafish had an orthologue the human genome (Howe et al. 2013), making it a useful model for studying *in vivo* biology. Zebrafish had a genome duplication event and therefore often have multiple copies of genes. For example, four isoforms of Cx36 exist, with two of them (Cx35.5 and Cx34.1) that account for the majority of Cx36 found in the larval brain (Miller et al. 2017). Cx35.5 (encoded by *gjd2a)* is present at the presynaptic terminal and Cx34.1 (encoded by *gjd1a*) is localized at the postsynaptic terminal. Both are required for electrical synapse formation and loss of *cx35.5*, specifically, results in a drastic reduction in all

isoforms of Cx36(Miller et al. 2017). We have acquired a Cx35.5 null Zebrafish mutant, which allows us to examine a functional Cx36 knock-out and those implications (Miller et al. 2017).

1.7 Chapter Summary

Neuronal communication is integral to the functioning of the brain and the organism. Different types of communication exist with each serving its purpose. Excitatory and inhibitory chemical neurotransmitters serve opposing roles in the determination of action potential firing, while gap junctions can influence and augment each of those roles through a direct connection to the extracellular space and other cells. The finite balance of excitation and inhibition is important for maintaining homeostasis within the brain and even slight disruptions can lead to seizures and epilepsy. The zebrafish is a great model for examining brain activity, gap junction dynamics, seizures, and epilepsy due to the various genetic and imagining tools that exist. Due to its small size, whole-brain effects can be elucidated, providing an opportunity to discover unexplored brain regions.

CHAPTER 2: REVIEW OF THE LITERATURE

2.1 Connexins

Connexins are transmembrane proteins that oligomerize to form a transmembrane pore called a hemichannel, which enables the exchange of molecules between the extracellular space and cell interior. Two hemichannels between adjacent cells can dock and form a continuous pore, known as a gap junction, allowing for direct intercellular coupling.

Several types of connexin proteins are expressed within the brain, both in non-neuronal cells and neurons. Connexin 43 (Cx43) is expressed in astrocytes and plays an important role in ion homeostasis at the synapse (Ca^{2+} and K^{+}) (Kofuji and Newman 2004; Cotrina et al. 1998). Through an interconnected network of Cx43-coupled astrocytes, ions can be shunted away from synapses and certain areas of the brain (Kofuji and Newman 2004). Dysfunction of this process may lead to the malfunction of neural networks. As such, Cx43 has been shown to play an important role in the development of epilepsy (Vincze et al. 2019). Connexin 36 (Cx36) is the main connexin expressed by neurons and forms inter-neuronal gap junctions (electrical synapses), which are responsible for fast synaptic transmission and the synchronous firing of neurons within the brain (Rash et al. 2012). It is involved in brain functions that rely on synchronous firing such as learning and memory (Wang and Belousov 2011; Allen et al. 2011), retina visual processing (Kovács-Öller et al. 2017), and sensorimotor reflex in the zebrafish (Miller et al. 2017). As the key structural component of electrical synapses, Cx36 may also act as a therapeutic target in diseases involving deficiencies in fast communication and aberrant synchronous firing, such as seizures. However, the reciprocal relationships between the Cx36 and seizures have remained unclear.

2.2 Connexin 36 and its effects on Epilepsy

Previous work has examined the roles of Cx36 in the pathogenesis of seizures, but there has been no consensus on whether Cx36 increases or decreases seizure susceptibility (Gajda et al. 2005; Jacobson et al. 2010; Shin 2013; Voss, Mutsaerts, and Sleigh 2010a). Jacobson et al. (2010) found that Cx36 knockout mice exhibited an increase in seizure-like behaviors following the administration pentylenetetrazol (PTZ; a GABA(A)-receptor antagonist), indicating that normal expression of Cx36 may be protective against seizure-inducing conditions. However, this finding contradicts studies using the connexin blocking drug quinine, which found the drug either decreased the severity of seizures (Gajda et al. 2005) or showed no change (Voss, Mutsaerts, and Sleigh 2010b). The discrepancy may potentially be due to the difference between chronic Cx36 deficiency (Cx36 knockout) versus acute Cx36 deficiency (quinine). However, quinine has broad antagonistic activity against many different connexins expressed in the nervous system, and the effects cannot be attributed solely to the inhibition of Cx36 (Manjarrez-Marmolejo and Franco-Pérez 2016; Cruikshank et al. 2004). Additionally, the difference in seizure induction methods and seizure metrics also makes direct comparisons between studies problematic.

2.3 Epilepsy and its effects on Connexin 36

Previous findings are also mixed regarding how neuronal hyperactivity affects the expression of Cx36. In rodent seizure models and epilepsy patient post-mortem samples, some groups have found that Cx36 expression was increased (Collignon et al., 2006; Laura, Xóchitl, Anne, & Alberto, 2015; X. Wu, Wang, Hao, & Feng, 2017), while others found decreased Cx36 expression (Condorelli et al. 2003; Söhl et al. 2000) or no change (Motaghi et al. 2017). Furthermore, even though seizures result in brain-wide changes in neuronal connectivity (Morgan, Gore, and Abou-Khalil 2010), seizure-induced changes in Cx36 expression had only been

examined in the dorsal telencephalon (cortex and hippocampus) (Condorelli et al. 2003; Laura et al. 2015; Motaghi et al. 2017; X. L. Wu et al. 2018). Potential changes to Cx36 expression in other brain areas following neuronal hyperactivity remain unknown.

2.4 Zebrafish and whole-brain activity mapping

To further investigate the relationship between Cx36 and neuronal hyperactivity and address the technical limitations listed above, we employ zebrafish as an experimental system. The small size of zebrafish larvae facilitates imaging of the whole brain under a laser scanning confocal microscope, which provides a unique opportunity to examine whole-brain activity as well as Cx36 protein regulation in an intact vertebrate organism. Additionally, the PTZ-induced seizure model in zebrafish has been well-characterized physiologically and behaviorally and is an effective model in identifying therapeutics to target epilepsy in humans (Baraban, Dinday, and Hortopan 2013; Baxendale et al. 2012). Previous studies using rodents and zebrafish have examined the diverse effects of PTZ in different brain regions (Baraban et al. 2005; Liu and Baraban 2019; Diaz Verdugo et al. 2019; Baxendale et al. 2012; Yang et al. 2019; Szyndler et al. 2009; Shehab et al. 1992; Nehlig 1998). These region-specific effects can be effectively captured in the zebrafish using a recently developed MAP-map technique utilizing phosphorylated extracellular-signal-regulated kinase (pERK) as a proxy for neuronal activity. (Randlett et al. 2015).

In zebrafish, Cx36 proteins are encoded by four genes: *cx35.1, cx34.7, cx34.1*, and *cx35.5* (Miller et al. 2017). In culture, all four isoforms are recognized by an anti-human Cx36 antibody, and the loss of either *cx34.1* or *cx35.5* resulted in the greatest reduction in brain-wide Cx36 antibody labeling. In contrast, loss of *cx34.7* and *cx35.1* have minimal effects on global Cx36 levels. Interestingly, the expression of Cx34.1 and Cx35.5 are mutually dependent. For example,

in the *cx35.5* loss-of-function animals (*cx35.5-/-*), the majority of anti-Cx36 labeling is lost, with weak residual labeling from Cx34.1(Miller et al. 2017).

Using zebrafish, we created a whole-brain activity map following hyperactivity using the MAP-mapping method (Randlett et al. 2015) to determine that there are both dose-varying and region-specific changes in neuronal hyperactivity following administration of PTZ. Additionally, we created a whole-brain expression map of Cx36 following the administration of PTZ. With this, we determined specific brain regions that showed decreases in Cx36 expression following hyperactivity. Finally, by acutely reducing the function of Cx36 using the Cx36 blocking drug, mefloquine, we determined that acute inhibition of Cx36 is detrimental, and leaves the animal more susceptible to PTZ-induced hyperactivity than their untreated counterparts.

CHAPTER 3: METHODS

3.1 Zebrafish Husbandry

All zebrafish used in this study were pigmentless (*nacre-/-*) in a mixed background of AB and TL wild-type strains (Zebrafish International Resource Center). *cx35.5* (ZFIN gene symbol: *gjd2a*) heterozygotes were gifts from Dr. Adam Miller at the University of Oregon. The Cx35.5 mutant was generated by TALEN-mediated genome targeting, which generated a frameshift mutation (5 bp deletion in exon 1) and polypeptide truncation (Shah et al. 2015). Zebrafish embryos and larvae were raised under 14 h light/10 h dark cycle at 28.5°C in water containing 0.1% Methylene Blue hydrate (Sigma-Aldrich). Sex is not a relevant variable for the larval stages being used (0-6 days post-fertilization, dpf), as laboratory zebrafish remain sexually undifferentiated until two weeks of age (Maack and Segner 2003; Wilson et al. 2014). All husbandry procedures and experiments were performed according to protocols approved by the Institutional Animal Care and Use Committee at Virginia Tech.

3.2 Immunohistochemistry

Zebrafish larvae were fixed overnight in 4% paraformaldehyde (PFA) on a rocker at 4°C. Samples were then processed and stained as previously described by Randlett et al. (2015). Primary antibodies that were used are as follows: p44/42 MAPK (tERK) (L34F12, Cell Signaling Technologies), Phospho-p44/42 MAPK (pERK) (D13.14.4E, Cell Signaling Technologies), and Anti-activated Caspase 3 (BD Pharmingen). For the Connexin antibody (36/GJA9, Invitrogen), fish were fixed in 2% TCA for 3 hours, and sample processing and staining were performed as previously described (Marsh et al. 2017).

3.3 MAP-map (Activity Map):

Wild-type and *cx35.5* mutant in 6 dpf zebrafish larvae were first acclimated for 15 minutes in a 6-well plate and then transferred into a well containing 0 mM (E3 embryo media only), 2 mM, 5 mM, 10 mM, or 20 mM PTZ in embryo media for 15 minutes. Larvae were then fixed in 4% PFA overnight and immunostained and imaged using a Nikon A1 confocal microscope. Subsequent MAP-mapping analysis was performed as previously described (Randlett et al. 2015) See Figure 3.1 for a representation of the analysis process. Brain regions highlighted in the text of this document were selected based on the following criteria: only brain regions were selected (individual neuron clusters were not mentioned), and only brain regions with well-defined functions were selected to be highlighted (See figure 3.2 for a representative brain atlas). All identified brain regions and neuron clusters can be found in the Supplementary tables.

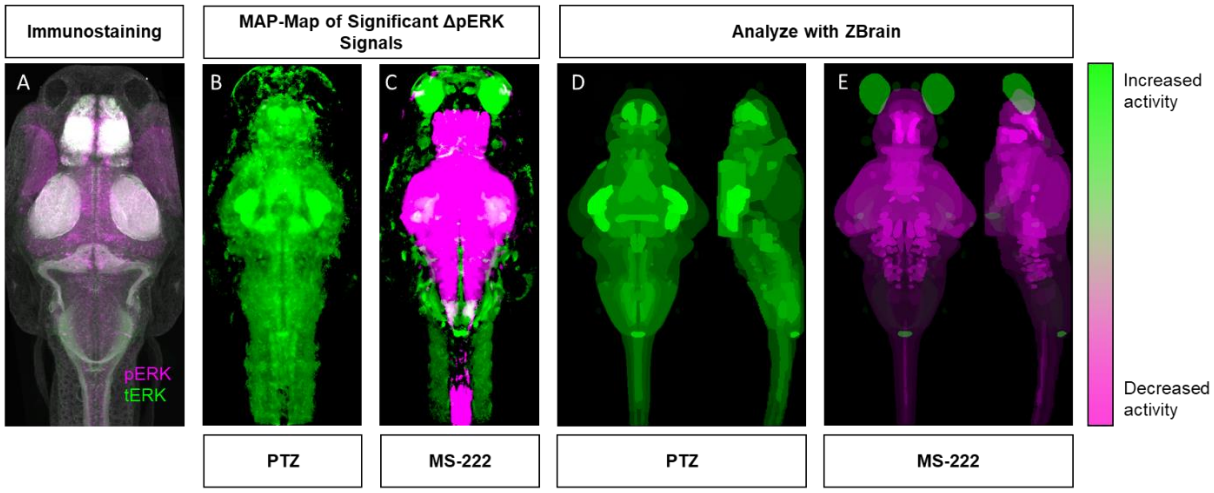

Adapted from Randlett et al, 2015

Figure 3.1. Representation of MAP-map analysis. A) Representative image of pERK (pink) and tERK (green) staining in a dorsal view of a zebrafish larvae. B) Images showing significant voxels of increased (green) activity or decreased (pink) activity in PTZ (seizure causing drug, left) or MS-222 (Anesthetic, right). C) Image showing identified ROI's with increased (green) or decreased (pink) activity in PTZ (left) or MS-222 (right). Adapted from Randlett et al., 2015.

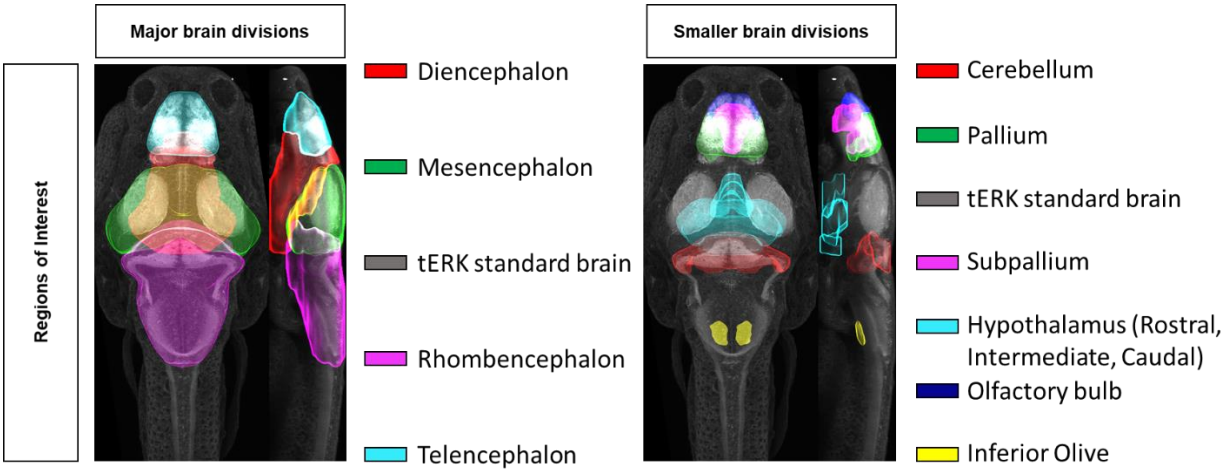
Regions of Interest
Major brain divisions
Diencephalon
Mesencephalon
tERK standard brain
Rhombencephalon
Telencephalon
Smaller brain divisions
Cerebellum
Pallium
tERK standard brain
Subpallium
Hypothalamus (Rostral, Intermediate, Caudal)
Olfactory bulb
Inferior Olive

Figure 3.2. Representative zebrafish brain atlas. Each brain region listed in this figure is mentioned in the text below as an ROI with statistically significant differences in neuronal activity, us this figure to refer back to when determining the location of activity changes in the zebrafish brain.

3.4 Cx36 Expression Map:

6 dpf larvae were acclimated for 15 minutes in a 6-well plate with embryo media and then transferred into a well containing 20 mM PTZ for either 30 minutes or 1 hour. Larvae were then either fixed immediately or allowed to recover for 1 hour, 3 hours, 6 hours, or 24 hours in embryo media. Larvae were fixed in 2% trichloroacetic acid (TCA) for 3 hours and immunostained as previously described (Miller et al. 2017). Confocal images were then morphed to a tERK standard brain image stack using CMTK (Randlett et al. 2015). To subtract background signal, an average stack of *cx35.5-/-* fish morphed and stained in the same way was subtracted from all images and then were processed as previously described, except for replacing pERK with the morphed and background subtracted anti-Cx36 (Randlett et al. 2015).

3.5 Cell Death Quantification:

6 dpf mutant and wild-type larvae were first acclimated for 15 minutes in a 6-well plate and then transferred into a well containing either embryo medium or 20 mM PTZ for 1 hour. Larvae were then immediately fixed in 4% PFA overnight, and immunostained Images were morphed to a standard brain and analyzed as previously described (Randlett et al. 2015). ROIs for the Diencephalon, Mesencephalon, Telencephalon from ZBrain were then overlaid on each stack, and Caspase positive cells were counted in each ROI. Standard unpaired t-tests with Holm-Sidak's correction for multiple comparisons were run between each group in GraphPad Prism.

3.6 Mefloquine Treatment:

At 6 dpf, larvae were exposed to either 0.025% DMSO (vehicle group) or 25 µM mefloquine. After 3 hours of exposure, fish and their relative media (either DMSO or mefloquine) were transferred to a 6 well plate and allowed to acclimate for 15 minutes. Larvae were then transferred to embryo media with 0 mM, 2 mM, 5 mM, 10 mM, or 20 mM PTZ for 15 minutes.

Larvae were then immediately fixed in 4% PFA overnight, immunostained, and imaged using a Nikon A1 confocal microscope. Subsequent analysis was performed as previously described (Randlett et al. 2015).

3.7 Image Processing and Statistical Analysis:

Images were processed and quantified using Fiji (Schindelin et al., 2012). MATLAB 2019 (MathWorks) was used for MAP-mapping analysis (Randlett et al., 2015). For Caspase-3 quantification, statistical analyses were performed in GraphPad Prism (Version 8). An unpaired t-test with Holm-Sidak's correction for multiple comparisons was performed. Results were considered significant if $p<0.05$.

All raw data will be available upon reasonable request.

CHAPTER 4: RESULTS

4.1 PTZ induces brain-wide neuronal hyperactivation in a dose-dependent manner.

PTZ inhibits GABA(A) receptor-mediated inhibitory neurotransmission, which leads to global neuronal hyperactivation and seizure-like neurological and behavioral phenotypes in both rodents and zebrafish (Baraban et al. 2005). To determine whether different brain regions have distinct sensitivities to PTZ-induced neuronal hyperactivation, we first compared whole-brain activity maps in wild-type fish exposed to varying concentrations of PTZ. To do this, we utilized the MAP-mapping assay to create whole-brain activity maps (Randlett et al. 2015). MAP-mapping offers a snapshot of neuronal activity by utilizing the ratio of the total extracellular signal-regulated kinase (tERK), which is present in all neurons, and phosphorylated ERK (pERK), the phosphorylated form of ERK that is induced (within 5 minutes (Cancedda et al. 2003; Ji et al. 1999; Dai et al. 2002)) following neuronal activity. The ratiometric pERK/tERK signal can then be quantified for individual, registered brain image stacks and statistically tested in an annotated 3D brain atlas (Z-Brain) (Randeltt et al. 2015). Statistical significance was determined through the Mann-Whitney U statistic, calculating statistically significant changes in the pERK/tERK ratio for each voxel. This is represented in each of the images to follow as statistically significant increases in pERK/tERK ratio shown in green and statistically significant decreases in pERK/tERK ratio shown in magenta. False discovery rate (FDR) correction was used with $p<0.00005$ as the cut off (Randlett et al. 2015). By averaging pERK across a large group of animals (7-20), MAP-map generates a spatially precise snapshot of average neuronal activity in a given group. This method allows us to assess the effects of PTZ on average neuronal activity, though the timing and location of ictal events cannot be determined due to the long temporal integration of ERK signaling.

Using MAP-mapping, we found region-specific changes in neuronal activity in response to varying concentrations of PTZ. We treated wild-type animals by bath-exposing them to embryo media with 2, 5, 10, and 20 mM PTZ for 15 minutes. Animals exposed to media only were used as the baseline for comparison. Neuronal activity was measured by the pERK/tERK ratio as described previously (Randlett et al. 2015). For a complete list of statistically significant changes by brain region in neuronal activity, see Supplementary Table 2. After exposure to 2 mM PTZ, we saw moderate increases in neuronal activity in more restricted brain areas in regions responsible for homeostatic regulation (hypothalamus and preoptic area) and executive functioning (subpallium, pallium) as well as the cerebellum (Figure 4.1A), see Figure 3.2 for an atlas of zebrafish brain regions. After exposure to 5, 10, and 20 mM PTZ, we observed broader increases in brain-wide neuronal activity (Figure 4.1B-D). These regions include those that were activated by 2 mM PTZ (hypothalamus, preoptic area, subpallium, and in many regions involved in movement control such as the pretectum, cerebellum, and oculomotor nuclei. Additionally, we observed some brain areas that became less active after exposure to PTZ: the telencephalon was less active at 10 and 20 mM PTZ than at lower concentrations (Figure 4.12D) and the olfactory bulb was less active across all PTZ concentrations (Figure 4.12A-D). The complete list of all identified changes is provided in Supplementary Table 1.

Overall, we were able to generate a PTZ dose-varying whole-brain activity map in 6 dpf zebrafish. We saw increased neuronal activity in areas previously identified to be involved in PTZ induced hyperactivity such as the pallium and optic tectum (Liu and Baraban 2019). We also identified additional regions that were previously unidentified such as the hypothalamus.

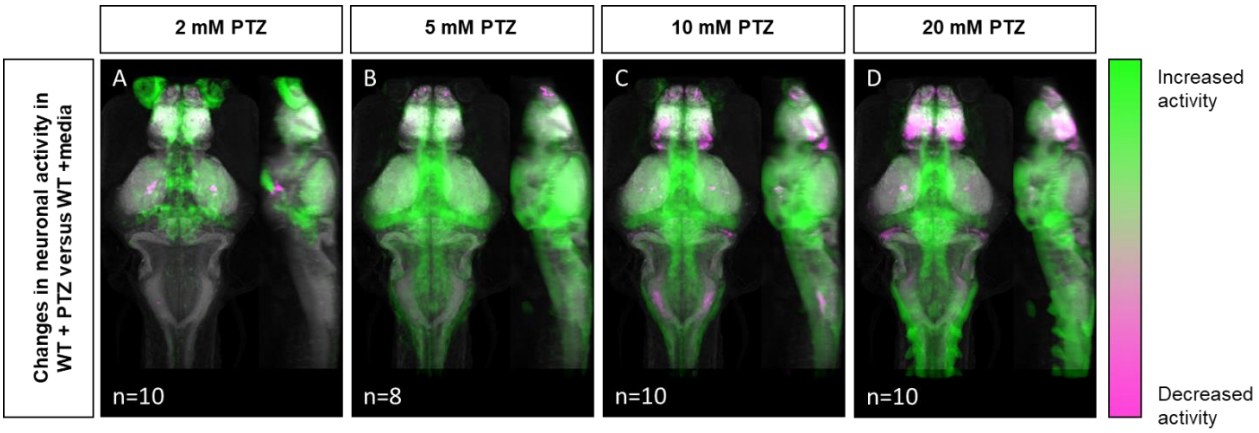
2 mM PTZ
5 mM PTZ
10 mM PTZ
20 mM PTZ
Changes in neuronal activity in WT + PTZ versus WT +media
A
B
C
D
n=10
n=8
n=10
n=10
Increased activity
Decreased activity

Figure 4.1. Whole-brain activity map showing significant regional differences in neuronal activity following various PTZ concentration exposure in wild-type zebrafish larvae. Dorsal and lateral view of zebrafish larvae brain. Colors indicate ROIs with higher pERK/tERK ratio in wild-type PTZ treated (green) or in Embryo Media (magenta) in A) 2 mM PTZ treated (n=10) B) 5 mM PTZ treated (n=8) C) 10 mM PTZ treated (n=10) and D) 20 mM PTZ treated (n=10) vs Embryo Media (n=10). Images show pixels with a significantly increased pERK/tERK ratio for treated fish (green) and untreated fish (magenta). For all regions $p < 0.005$

4.2 Genetic *cx35.5* deficiency results in changes in PTZ-induced brain-wide neuronal hyperactivity

To understand what effect loss of Cx36 has on hyperactivity we examined whole-brain activity changes at different concentrations of PTZ in the *cx35.5-/-* larvae. *cx35.5-/-* mutant fish show complete loss of the *cx35.5* isoform of Cx36 as well as a significant reduction *cx34.1*, however, some residual *cx34.1* remains and the mutant is, therefore, not a full knock-out of all Cx36 isoforms. (Miller et al., 2017 and also Figure 4.5B). We again employed the MAP-mapping technique to determine which brain regions show a significant difference between PTZ-treated mutants and untreated mutants. Similar to their wild-type siblings, at 2 mM PTZ, significant increases in neuronal activity in the diencephalon (preoptic area and hypothalamus) and telencephalon (subpallium), were observed (Figure 4.2A), see Figure 3.2 for an atlas of zebrafish brain regions. Additionally, we saw increases in the diencephalon (retinal arborization fields) associated with visual processing (Figure 4.2A). At 5, 10, and 20 mM PTZ, we found a very similar map to that of their wild-type siblings, with increases and decreases in many of the same major brain regions listed previously (Figure 4.2 B-D). For a complete list of significantly change brain regions, see Supplementary Table 1.

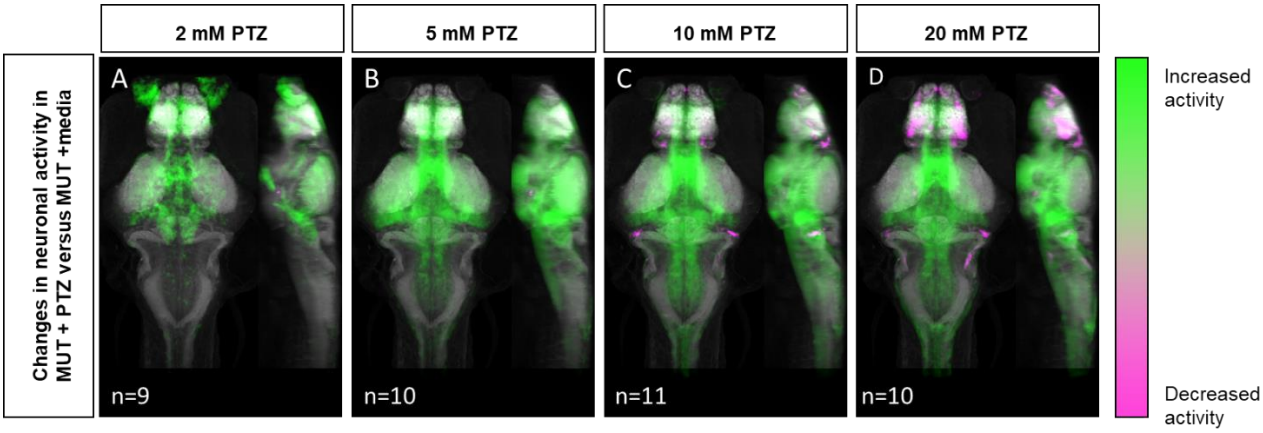
2 mM PTZ
5 mM PTZ
10 mM PTZ
20 mM PTZ
Changes in neuronal activity in MUT + PTZ versus MUT +media
A
B
C
D
n=9
n=10
n=11
n=10
Increased activity
Decreased activity

Figure 4.2. Whole-brain activity map showing significant regional differences in neuronal activity following various PTZ concentration exposure in *cx35.5-/-* zebrafish larvae. Dorsal and lateral view of zebrafish larvae brain. Colors indicate ROIs with higher pERK/tERK ratio in *cx35*.5 -/- larvae PTZ treated (green) or in Embryo Media (magenta) in A) 2 mM PTZ treated (n=9) B) 5mM PTZ treated (n=10) C) 10mM PTZ treated (n=11) and D) 20mM PTZ treated (n=10) vs Embryo Media (n=9). Images show pixels with a significantly increased pERK/tERK ratio for treated fish (green) and untreated fish (magenta). For all regions $p < 0.005$

4.3 Changes in *cx35.5-/-* whole-brain activity maps compared to wild-type

To understand differences in neuronal hyperactivity between *cx35.5 -/-* and wild-type animals, we compared the activity map of *cx35.5-/-* and wild-type siblings at baseline (media only) and after exposure to different concentrations of PTZ (Figure 4.1A-D). We observed no increases in neuronal activity at baseline, however, we did observe decreases in activity in *cx35.5-/-* relative to wild-type in the rhombencephalon reticulospinal neurons and medial vestibular neurons (Figure 4.3A), see Figure 3.2 for an atlas of zebrafish brain regions. At 2 mM PTZ, there were no significant changes in brain-wide neuronal activity between *cx35.5-/-* and wild-type siblings (Figure 4.3B). At 5 mM PTZ, there were small increases in activity in the diencephalon (hypothalamus) and the telencephalon (subpallium) (Figure 4.3C). At 10 mM PTZ, we observed increases in the hypothalamus and various regions within the rhombencephalon (Figure 4.3D). We also found regions that show less of an increase in activity in *cx35.5-/-* compared to wild-type within the rhombencephalon specifically in regions that rely on the synchronous firing capabilities of Cx36 (Mauthner cells, inferior olive) (Yao et al. 2014; Flores et al. 2012; Bazzigaluppi et al. 2017). At the highest concentration (20 mM), we saw increased activity in the *cx35.5-/-* compared to wild-type in areas previously identified as associated with seizures in the telencephalon such as the pallium (Liu and Baraban 2019) as well as the hypothalamus. These regions are similar to our findings in the wild-type animals after PTZ exposure, indicating an increase in severity of hyperactivity in these regions following treatment with PTZ in *cx35.5-/-* animals. We also observed regions that show fewer increases in activity in the rhombencephalon, relative to wild-type, similar to 10 mM PTZ, but they are less severe (Figure 4.3 D, E). For a complete list of regional differences, please see Supplementary Table 1.

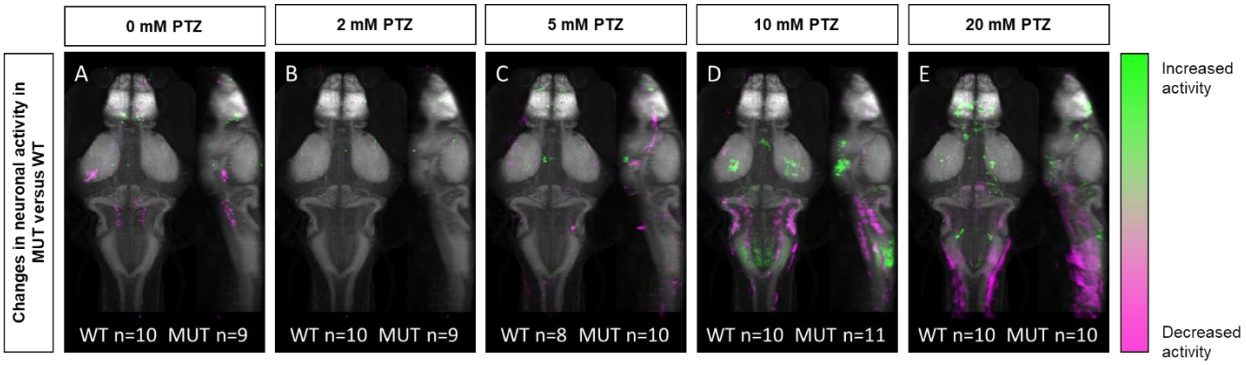
0 mM PTZ
2 mM PTZ
5 mM PTZ
10 mM PTZ
20 mM PTZ
Changes in neuronal activity in MUT versus WT
A
B
C
D
E
WT n=10 MUT n=9
WT n=10 MUT n=9
WT n=8 MUT n=10
WT n=10 MUT n=11
WT n=10 MUT n=10
Increased activity
Decreased activity

Figure 4.3. Whole-brain activity map showing significant regional differences in neuronal activity following various PTZ concentration exposure in *cx35.5-/-* versus wild-type zebrafish larvae. Dorsal and lateral view of zebrafish larvae brain. Colors indicate ROIs with higher pERK/tERK ratio in *cx35.5-/-* (green) or wild type (magenta) in A) E3 treated (WT n=10, MUT n=9) B) 2 mM PTZ treated (WT n=10, MUT n=9) C) 5 mM PTZ treated (WT n=8, MUT=10) D) 10 mM PTZ treated (WT n=10, MUT n=11) and E) 20 mM PTZ treated (WT n=10, MUT n=10) *cx35.5-/-* vs WT. Images show pixels with significantly increased pERK/tERK ratio for treated fish (green) and untreated fish (magenta). For all regions $p < 0.005$

4.4 Genetic *cx35.5* deficiency does not affect cell death at baseline or after PTZ

We determined that PTZ alone and PTZ in combination with *cx35.5* deficiency resulted in regional and dose-varying changes in whole-brain neuronal activity. One possible explanation is that *cx35.5* mutation may result in altered neuronal cell death, either at baseline or after PTZ, which would then alter the overall balance of brain-wide connectivity. To test this, we stained for activated caspase-3 (a marker of apoptotic cells) and quantified the number of positive cells in each of the major brain divisions (rhombencephalon, mesencephalon, telencephalon, and diencephalon, see Figure 3.2 for an atlas of zebrafish brain regions). We found that there were no differences at baseline (media only) in the number of caspase-3 positive cells between *cx35.5-/-* and wild-type siblings in any of the major brain divisions (Figure 4.4A, B, D, E). Additionally, no difference in the number of caspase-3 positive cells when comparing both *cx35.5-/-* and wild-type siblings after 20 mM PTZ was found (Figure 4.4C, F). From these data, we, therefore, conclude that changes in neuronal response in *cx35.5* animals are not likely caused by altered cell death induction.

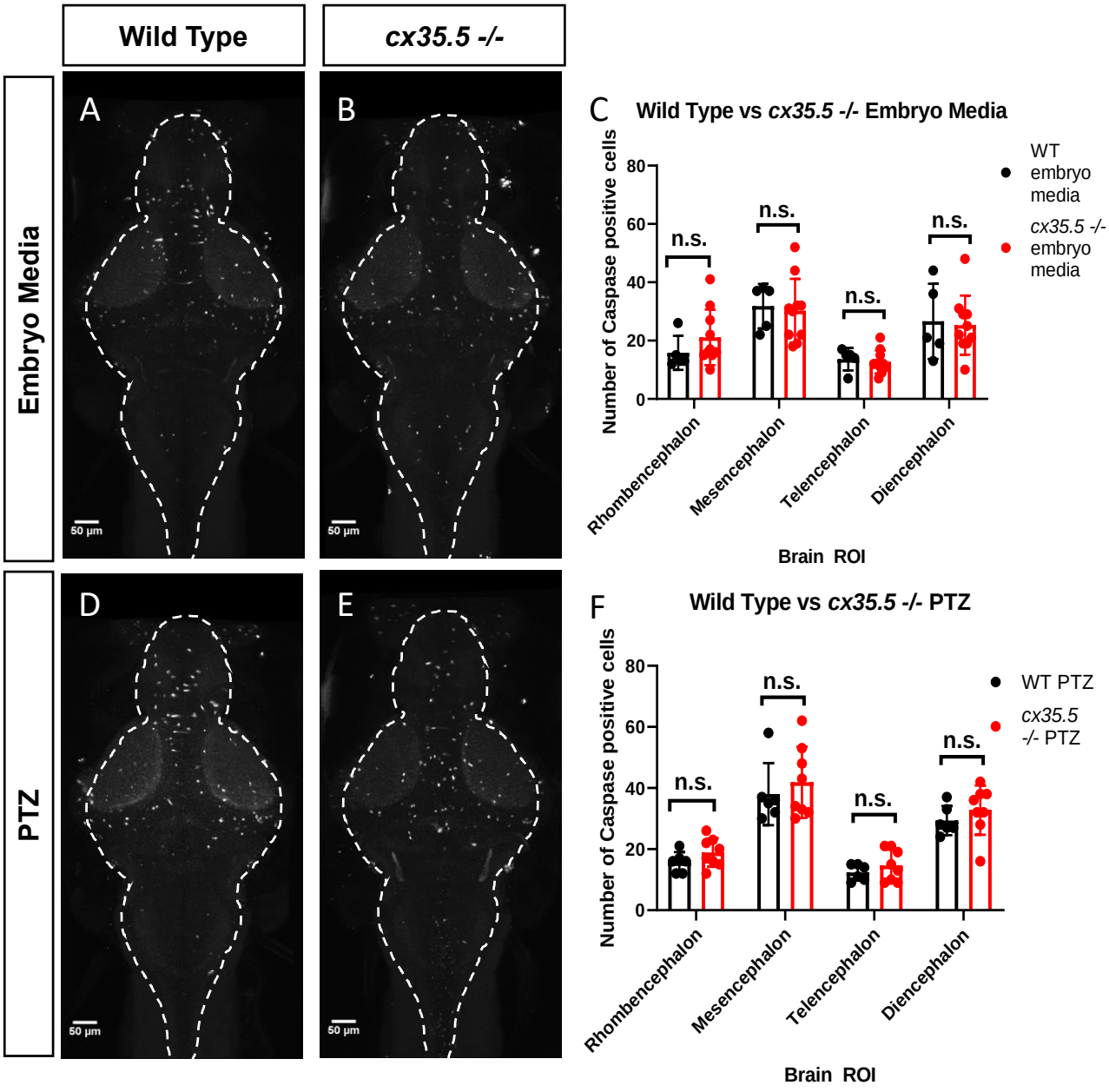
Wild Type
cx35.5 -/-
Embryo Media
PTZ
A
B
D
E
50 µm
C
Wild Type vs cx35.5 -/- Embryo Media
Number of Caspase positive cells
n.s.
Rhombencephalon
Mesencephalon
Telencephalon
Diencephalon
Brain ROI
WT embryo media
cx35.5 -/- embryo media
F
Wild Type vs cx35.5 -/- PTZ
WT PTZ
cx35.5 -/- PTZ

Figure 4.4. Caspase positive cells by major brain division, comparing cx35.5-/- vs wild type with and without PTZ. Representative images (Caspase-3 staining) A, B, D, E. C) A graph depicting the number of Caspase-3 positive cells in the Rhombencephalon, Mesencephalon, Telencephalon, and Diencephalon in wild-type (black) vs cx35.5-/- (red) fish with treatment with F) Embryo medium (Vehicle) or F) PTZ. Data were analyzed using a student's t-test with Holm-Sidak's correction for multiple comparisons. Embryo medium (vehicle) treatment, wild type n=5, cx35.5-/- n= 10. PTZ treatment, wild type n= 6 cx35.5-/- n=8.

4.5 Creation of the whole-brain Cx36 expression map

To understand how neuronal hyperactivity affects Cx36, we created a whole-brain *expression* map to efficiently, and in a non-biased manner, measure changes in protein expression using a modified MAP-mapping processing procedure. We utilized a previously-validated human anti-Cx36 antibody that recognizes all four isoforms of Cx36 in the zebrafish (*cx34.7*, *cx35.1*, *cx34.1*, and *cx35.5*). The antibody was validated against zebrafish-specific and isoform-specific generated antibodies in HeLa cells (Miller et al. 2017). Using this antibody, we stained wild-type (Figure 4.5A) and *cx35.5-/-* (Figure 4.5B) siblings. Consistent with previous studies, significant loss of anti-Cx36 staining in *cx35.5-/-* animals was detected (Figure 4.5A, B). To quantify Cx36 expression across the whole brain, we performed image normalization (with CMTK) and subtracted the average stack of all *cx35.5-/-* fish from each animal. We then followed the same MAP-mapping processing pipeline to quantify the Cx36/tERK ratio. tERK staining is used for morphing as a standard, consistent (Figure 4.6) label and to normalize staining intensity across animals and conditions considering the sparse expression of Cx36. Statistical significance was determined through the Mann-Whitney U statistic, calculating statistically significant changes in the Cx36/tERK ratio for each voxel. This is represented in each of the images to follow as statistically significant increases in the Cx36/tERK ratio shown in cyan and statistically significant decreases in the Cx36/tERK ratio shown in red. FDR correction was used with $p<0.00005$ as the cut-off for significance. (Randlett et al. 2015). The resulting Cx36 expression map reveals decreases in Cx36 staining intensity in *cx35.5-/-* fish compared to wild-type siblings in regions such as the mesencephalon (optic tectum), rhombencephalon (rhombomeres, mauthner cells), etc. (Figure 3C). See Supplementary Table 2 for a complete list of regional changes. We then applied this same method to examine Cx36 expression after PTZ.

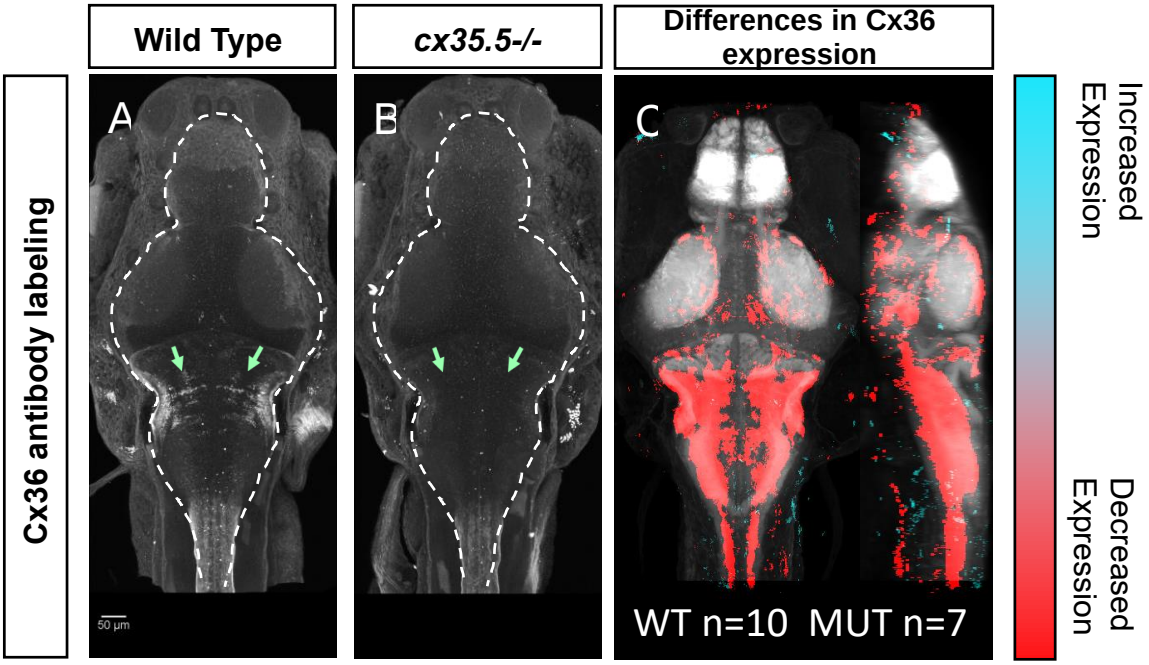
Wild Type
cx35.5-/-
Differences in Cx36 expression
Cx36 antibody labeling
A
B
C
50 µm
WT n=10 MUT n=7
Increased Expression
Decreased Expression

Figure 4.5. Whole-brain expression map of cx35.5-/- vs wild-type zebrafish larvae immunostaining of anti-human Cx36. Whole-brain expression of Cx36 using an anti-human Cx36 antibody vs tERK. Cyan indicates increases in fluorescence over tERK in cx35.5-/- fish, red indicates increases in fluorescence over tERK in wild-type fish A) Cx36 immunostaining of cx35.5 -/- fish B) Cx36 immunostaining of wild-type fish C) Dorsal and lateral view of zebrafish larvae brain. Whole-brain expression map showing increased expression in cx35.5-/- (cyan) and increased expression in wild type (red). Wild type n=10, cx35.5-/- n=7 $p<0.005$

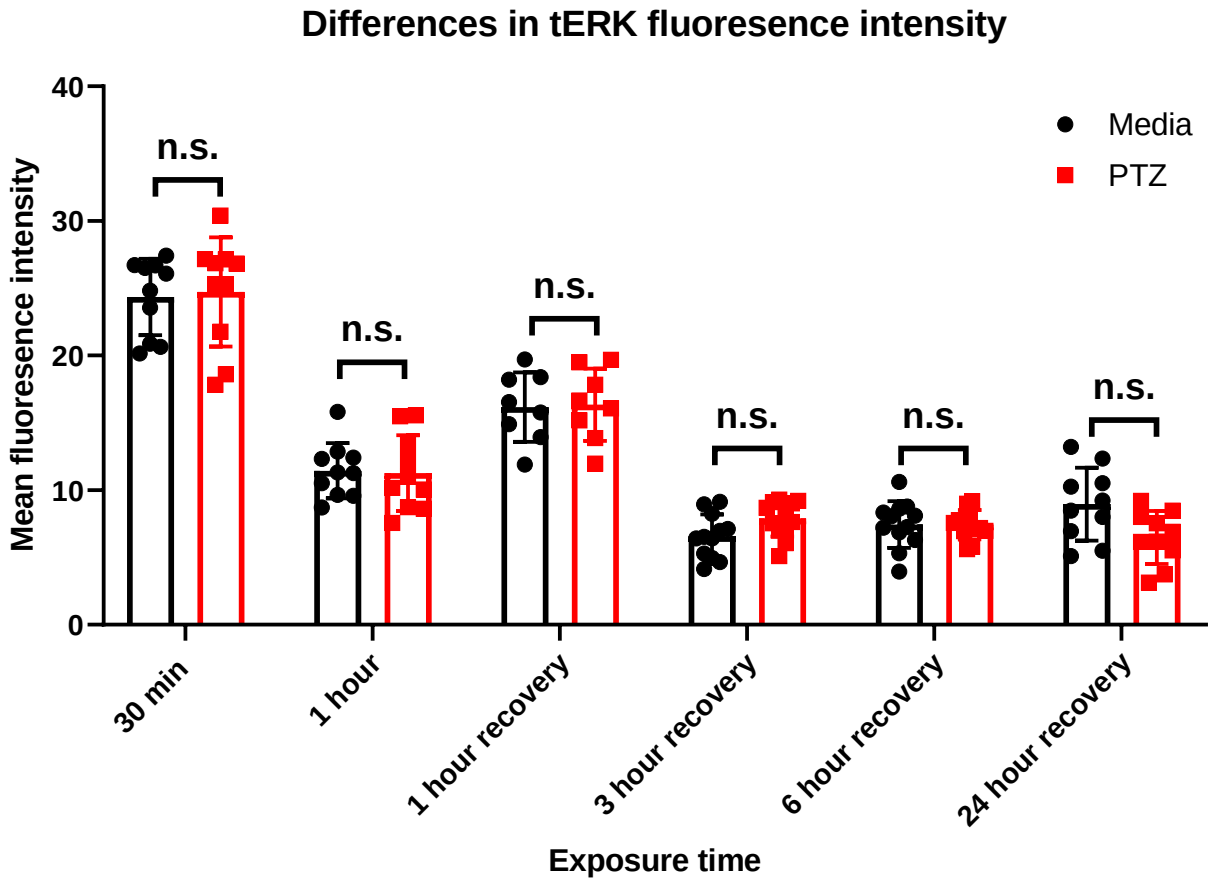
Differences in tERK fluoresence intensity
Mean fluoresence intensity
40
30
20
10
0
n.s.
n.s.
n.s.
n.s.
n.s.
n.s.
Media
PTZ
30 min
1 hour
1 hour recovery
3 hour recovery
6 hour recovery
24 hour recovery
Exposure time

Figure 4.6. Consistency in tERK staining intensity. Graph depicting consistency in mean tERK staining intensity between all Cx36 co-stained groups showing differences only between staining sessions.

4.6 Reduced Cx36 expression following PTZ exposure

Next, to determine if exposure to PTZ changes Cx36 expression, we compared the Cx36 expression map between PTZ-treated animals and untreated animals (media only). Due to the time-frame of Cx36 turnover (half-life of ~1-3 hours) (Flores et al. 2012), we did not expect to see changes in expression after only 15 minutes of PTZ exposure. As such, we exposed fish to PTZ for both 30 minutes and 1 hour to ensure we captured changes in expression. After 30 minutes of PTZ exposure, we found a global decrease in Cx36 labeling (Figure 4.7A). A similar but more pronounced effect was observed after 1 hour (Figure 4.7B). We saw decreases in Cx36 expression in the mesencephalon (optic tectum), the diencephalon (retinal arborization fields), and in the rhombencephalon in rhombomere 7, an area that is important for motor behavior (Figure 4.7A, B). After 1 hour of PTZ, there was also a decrease in expression within the cerebellum (Figure 4.7B), an area that relies heavily on Cx36 for synchronous firing. For a complete list of ROIs with changes, see Supplementary Table 2. Together, these data reveal that Cx36 expression is reduced following exposure to PTZ after 30 minutes, and this is exacerbated after 1 hour of exposure.

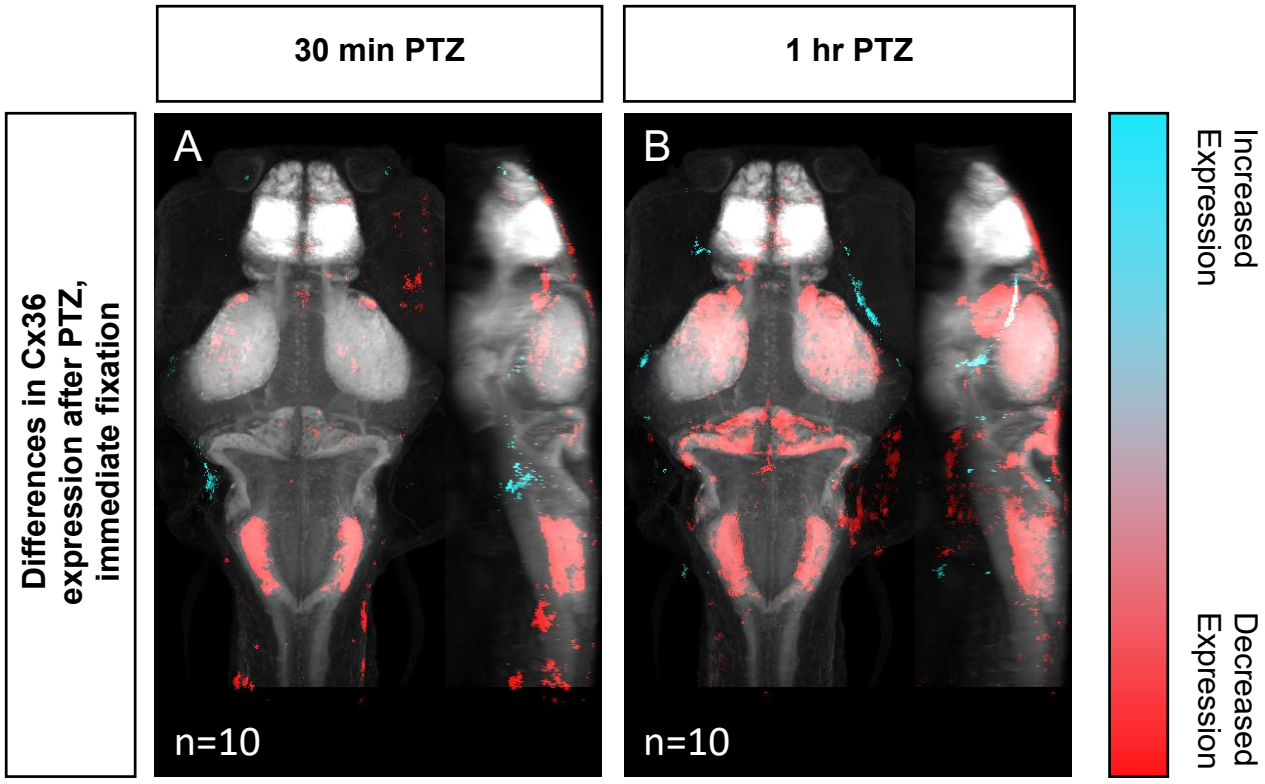
30 min PTZ
1 hr PTZ
Differences in Cx36 expression after PTZ, immediate fixation
A
B
n=10
n=10
Increased Expression
Decreased Expression

Figure 4.7. Wild type whole-brain immunostaining Cx36 expression map in E3 vs PTZ treated zebrafish larvae. Dorsal and lateral view of zebrafish larvae brain. Whole-brain expression of Cx36 using an anti-human Cx36 antibody vs tERK. Cyan indicates increases in fluorescence over tERK in PTZ treated fish, red indicates increases in fluorescence over tERK in E3 treated fish A) After 30 min of 20 mM PTZ exposure (n=10) B) After 1 hr of 20 mM PTZ exposure (n=10) C) 1-hour recovery after PTZ is removed, n=12 D) 3 hours of recovery after PTZ is removed, n=12 E) 6 hours of recovery after PTZ is removed, n=12 F) 24 hours of recovery after PTZ is removed, n=10. For all regions $p < 0.005$ G) A graph depicting the number of Caspase-3 positive cells in the Rhombencephalon, Mesencephalon, Telencephalon, and Diencephalon in wild-type fish with treatment with embryo medium (Vehicle) (Black) or PTZ (Red). Data were analyzed using a student's t-test with Holm-Sidak's correction, n=9.

4.7 Recovery of Cx36 expression following cessation of PTZ exposure

To test whether Cx36 expression recovers after the removal of PTZ, we created Cx36 expression maps for animals exposed to 20 mM PTZ for one hour and then allowed them to recover in embryo media for 1, 3, 6, or 24 hours after PTZ removal. Compared to animals not exposed to PTZ (media only), Cx36 expression was still significantly decreased in the telencephalon (pallium, subpallium) and diencephalon (habenula, pretectum), after 1 hour of recovery, but there were some increases in expression in restricted areas in the rhombencephalon (Figure 4.8A). The decrease in Cx36 expression was almost entirely recovered after 3 hours (Figure 4.8B). Interestingly, the expression is then slightly increased by 6 hours of recovery in the mesencephalon (optic tectum, neuropil), and the cerebellum (Figure 4.8C). This is maintained 24 hours later (Figure 4.8D). For a complete list of regions that show changes in expression, see Supplementary Table 2. These alterations in expression were not due to cell death resulting from long-term PTZ exposure as no significant differences in the number of caspase-3 positive cells in between untreated (media only) versus those treated with 20 mM PTZ for one hour (Fig. 4.8) we detected.

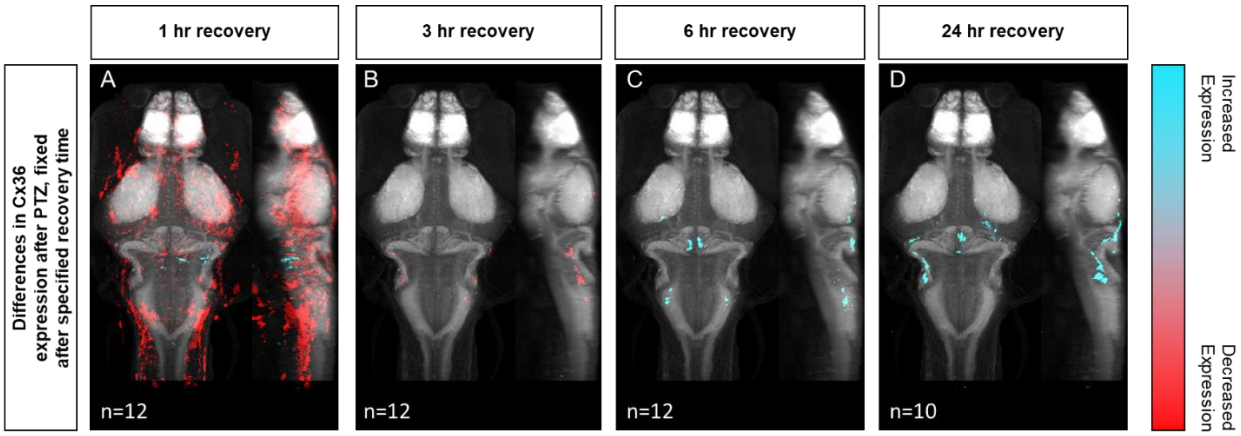
1 hr recovery
3 hr recovery
6 hr recovery
24 hr recovery
Differences in Cx36 expression after PTZ, fixed after specified recovery time
A
B
C
D
n=12
n=12
n=12
n=10
Increased Expression
Decreased Expression

Figure 4.8. Wild type whole-brain immunostaining Cx36 expression map in E3 vs PTZ treated zebrafish larvae. Dorsal and lateral view of zebrafish larvae brain. Whole-brain expression of Cx36 using an anti-human Cx36 antibody vs tERK. Cyan indicates increases in fluorescence over tERK in PTZ treated fish, red indicates increases in fluorescence over tERK in E3 treated fish after A) 1-hour recovery after PTZ is removed, n=12 B) 3 hours of recovery after PTZ is removed, n=12 C) 6 hours of recovery after PTZ is removed, n=12 D) 24 hours of recovery after PTZ is removed, n=10. For all regions $p < 0.005$

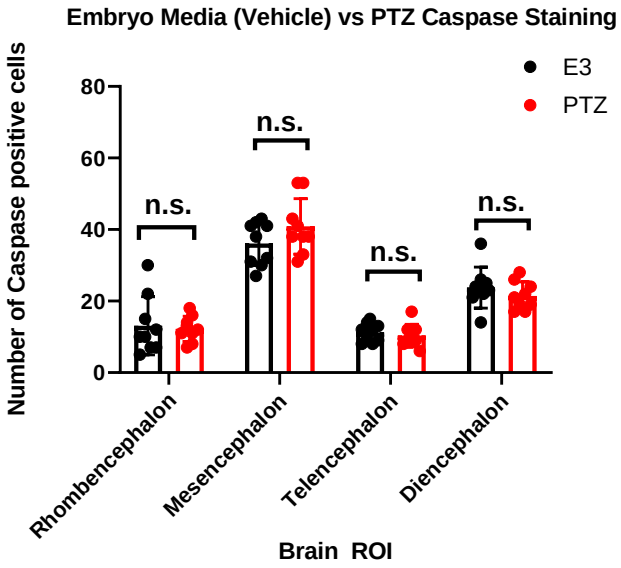
Embryo Media (Vehicle) vs PTZ Caspase Staining
E3
PTZ
Number of Caspase positive cells
80
60
40
20
0
n.s.
n.s.
n.s.
n.s.
Rhombencephalon
Mesencephalon
Telencephalon
Diencephalon
Brain ROI

Figure 4.9. Cell death after exposure to 20 mM PTZ. A graph depicting the number of Caspase-3 positive cells in the Rhombencephalon, Mesencephalon, Telencephalon, and Diencephalon in wild-type fish with treatment with embryo medium (Vehicle) (Black) or PTZ (Red). Data were analyzed using a student's t-test with Holm-Sidak's correction, n=9.

4.8 DMSO and mefloquine treated animals show a PTZ dose-dependent increase in neuronal activity

Given that PTZ-induced neuronal hyperactivity resulted in decreased Cx36 expression, we next tested whether the acute reduction of Cx36 function may contribute to further susceptibility to neuronal hyperactivation, i.e., whether PTZ-induced Cx36 reduction is maladaptive. To acutely inhibit Cx36 function, we utilized a Cx36-specific blocking drug, mefloquine, and examined changes in neuronal activity (Harris and Locke 2008). The effects of mefloquine were assessed by comparing the activity maps of wild-type fish treated with DMSO (vehicle) or 25 μM mefloquine for 3 hours before exposure to varying concentrations of PTZ (0-20 mM). Similar to our wild-type activity mapping (Figure 4.1A-D), we observed broad increases in neuronal activity in DMSO treated animals following exposure to PTZ in a dose-dependent manner (Figure 4.10A-D). These increases were greater compared to our animals not exposed to DMSO (Figure 4.1A-D, Figure 4.12), likely due to the mild inhibitory effects of DMSO (Figure 4.11, see Supplementary Table 5 for a full list of changed regions) on excitatory currents (Tamagnini et al. 2014; Lu and Mattson 2001). At 2-5 mM PTZ, we saw increases in activity in the mesencephalon (optic tectum, neuropil), rhombencephalon (cerebellum), telencephalon (pallium), and diencephalon (hypothalamus) (Figure 4.10 A-B, See figure 3.2 for referenced zebrafish brain regions). There were also decreases in activity in the olfactory bulb (Figure 4.10A). At 5 mM PTZ, we found increases in activity in similar regions as well as the mesencephalon (retinal arborization fields) and decreases in the olfactory bulb (Figure 4.10B). At 10 mM we observed increases in similar regions, with greater increases seen in the hypothalamus, decreases in the olfactory system and, small decreases in the hypothalamus and pallium (Figure 4.10C). Finally, at 20 mM PTZ increases in neuronal activity in similar regions as the previous doses were observed, with the greatest increases seen in the

hypothalamus. Decreases in the olfactory system, hypothalamus, and pallium (Figure 4.10D) were also observed. In fish treated with mefloquine, we found very similar overall patterns as the DMSO treated fish (Figure 4.10A-D), with progressively higher neuronal activity with increasing PTZ concentrations (Figure 4.10E-H).

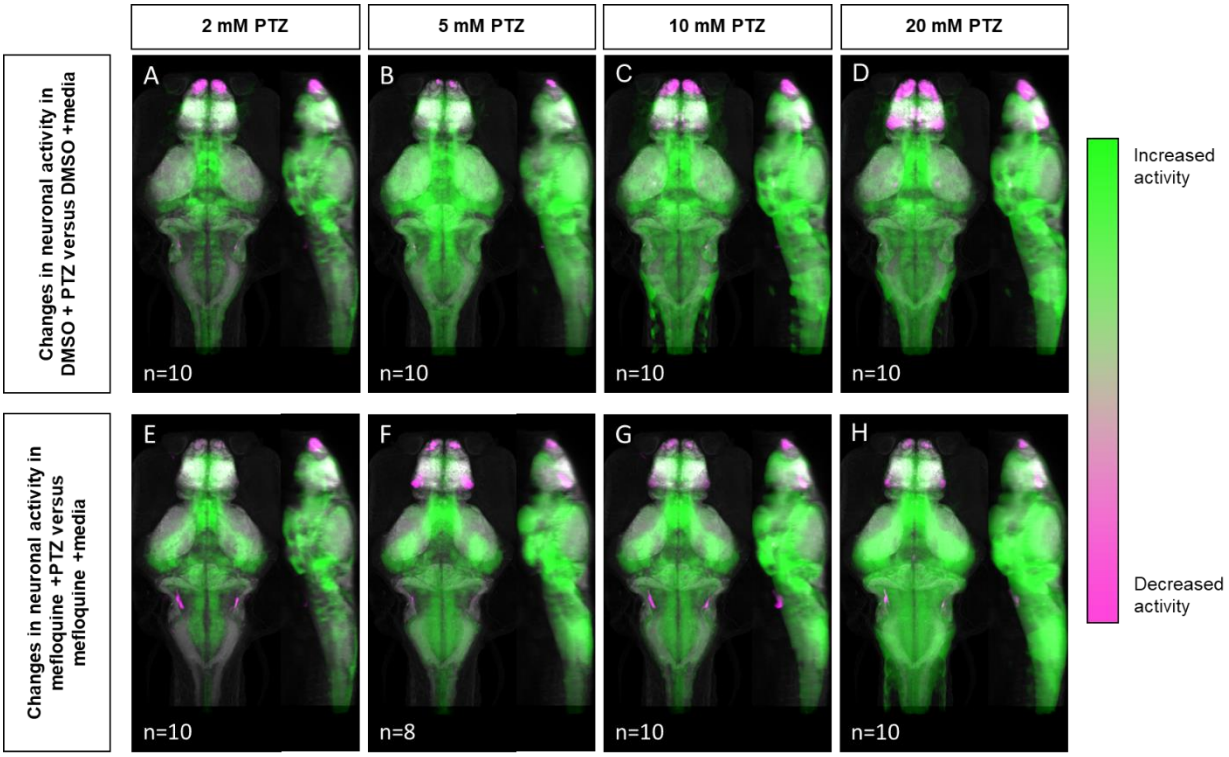
2 mM PTZ
5 mM PTZ
10 mM PTZ
20 mM PTZ
Changes in neuronal activity in DMSO + PTZ versus DMSO +media
Changes in neuronal activity in mefloquine +PTZ versus mefloquine +media
A
B
C
D
E
F
G
H
n=10
n=10
n=10
n=10
n=10
n=8
n=10
n=10
Increased activity
Decreased activity

Figure 4.10. Whole-brain activity map showing significant regional differences following Connexin 36 blocking drug mefloquine and PTZ exposure in wild-type zebrafish larvae. Dorsal and lateral view of zebrafish larvae brain. Images show pixels with significantly increased pERK/tERK ratio compared to DMSO and embryo medium (n=9) for DMSO treated fish after A) 2 mM PTZ (n=10) B) 5 mM PTZ (n=10) C) 10 mM PTZ (n=10) and D) 20 mM PTZ (n=10). E-H) Images show pixels with significantly increased pERK/tERK ratio compared to mefloquine and embryo medium treated fish (n=9) after E) 2 mM n=10) PTZ F) 5 mM PTZ (n=8) G) 10 mM PTZ (n=10) and H) 20 mM PTZ (n=10). For all regions $p < 0.005$

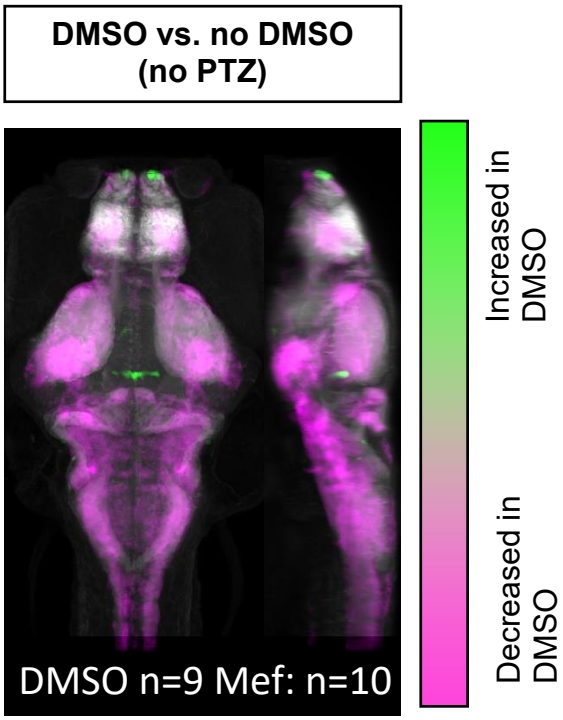
DMSO vs. no DMSO
(no PTZ)
DMSO n=9 Mef: n=10
Increased in DMSO
Decreased in DMSO

Figure 4.11. Whole-brain activity map showing off-target effects of DMSO in wild-type animals. Dorsal and lateral view of zebrafish larvae brain. Images show pixels with significantly increased pERK/tERK ratio in DMSO treated wild-type animals vs embryo media treated wild-type animals (DMSO n=9 Mef: n=10) For all regions $p < 0.005$

4.9 Acute blockade of Cx36 increases neuronal hyperactivity following PTZ exposure

Next, we compared mefloquine versus DMSO treated siblings at different concentrations of PTZ. In the absence of PTZ, the mefloquine treated fish showed increases and decreases in neuronal activity in different brain regions, compared to DMSO-treated siblings (Figure 4.12A). Specifically, we saw moderate increases in the hypothalamus, cerebellum, and mesencephalon (tegmentum). There were decreases in neuronal activity compared to DMSO-treated controls in the telencephalon, specifically in the olfactory bulb and subpallium (Figure 4.12B). At 2 mM PTZ, mefloquine treated fish showed increases in the major regions associated with PTZ exposure (Figure 4.1A), compared to DMSO-treated fish. Increases in the hypothalamus, diencephalon (retinal arborization fields, pretectum), and telencephalon (subpallium) were found. There were decreases in the olfactory bulb and other regions of the telencephalon (Figure 4.12B) compared to controls (Figure 4.12B). At 5 mM PTZ, we found similar regions of increased activity in mefloquine treated fish, but we also saw regions that showed decreased activity compared to control within both the telencephalon and the rhombencephalon (Figure 4.12C). Some rhombencephalon regions with decreased activity are known to rely on Cx36 functionality, specifically the inferior olive and Mauthner cells (Yao et al. 2014; Flores et al. 2012; Bazzigaluppi et al. 2017). At 10 and 20 mM PTZ, we observed similar increases in activity in mefloquine treated fish, each increasing with PTZ dose, and less of an increase in activity compared to control in the telencephalon, that was less severe than 10 mM, in these two groups (Figure 4.12D-E). At 20 mM we observed a decrease in activity in the hypothalamus and mesencephalon (oculomotor nuclei) compared to wild-type, which was not observed at other doses (Figure 4.12E). For a complete list of regions changed, see Supplementary Table 3.

Compared to cx35.5-/- animals (Figure 4.3A-D) the activity increases we found in the mefloquine-treated animals were more wide-spread. However, there is a high degree of overlap in the regions with increased activity at higher PTZ concentrations (Figure 4.13, Figure 4.14). Nearly all regions with increased neural activity in the mutants (65 out of 67 at 10 mM PTZ, 52 out of 53 at 20 mM PZ) showed increased activity in mefloquine treated animals. Overall, these results indicate that the acute reduction of Cx36 functionality results in increased susceptibility to PTZ-induced neuronal hyperactivity.

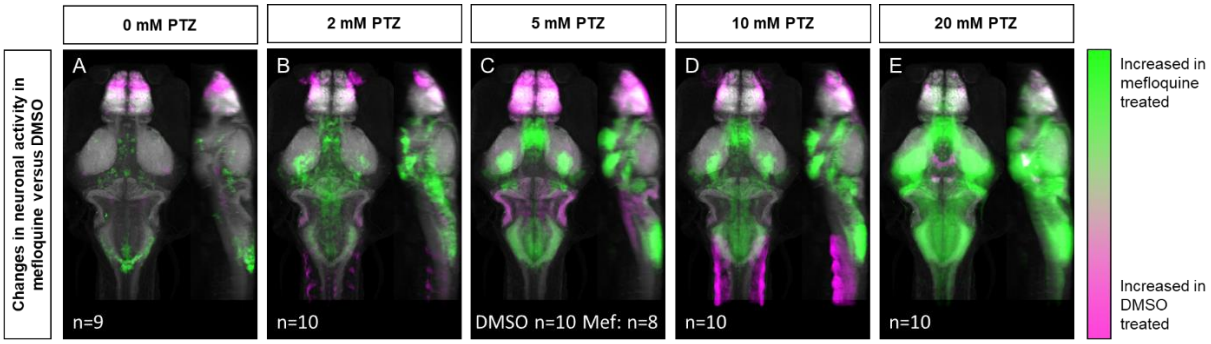
0 mM PTZ
2 mM PTZ
5 mM PTZ
10 mM PTZ
20 mM PTZ
Changes in neuronal activity in mefloquine versus DMSO
A
B
C
D
E
n=9
n=10
DMSO n=10 Mef: n=8
n=10
n=10
Increased in mefloquine treated
Increased in DMSO treated

Figure 4.12. Whole-brain activity map showing significant regional differences following Connexin 36 blocking drug mefloquine and PTZ exposure in wild-type zebrafish larvae. Dorsal and lateral view of zebrafish larvae brain. Images show pixels with significantly increased pERK/tERK ratio for mefloquine (25 μM) treated fish (green) and for DMSO (Vehicle) treated fish (magenta) after exposure to A) embryo medium (n=9) B) 2mM PTZ (n=10) C) 5 mM (DMSO n=10, mefloquine n=8) PTZ D) 10 mM PTZ (n=10) E) 20 mM PTZ (n=10). For all regions $p < 0.005$

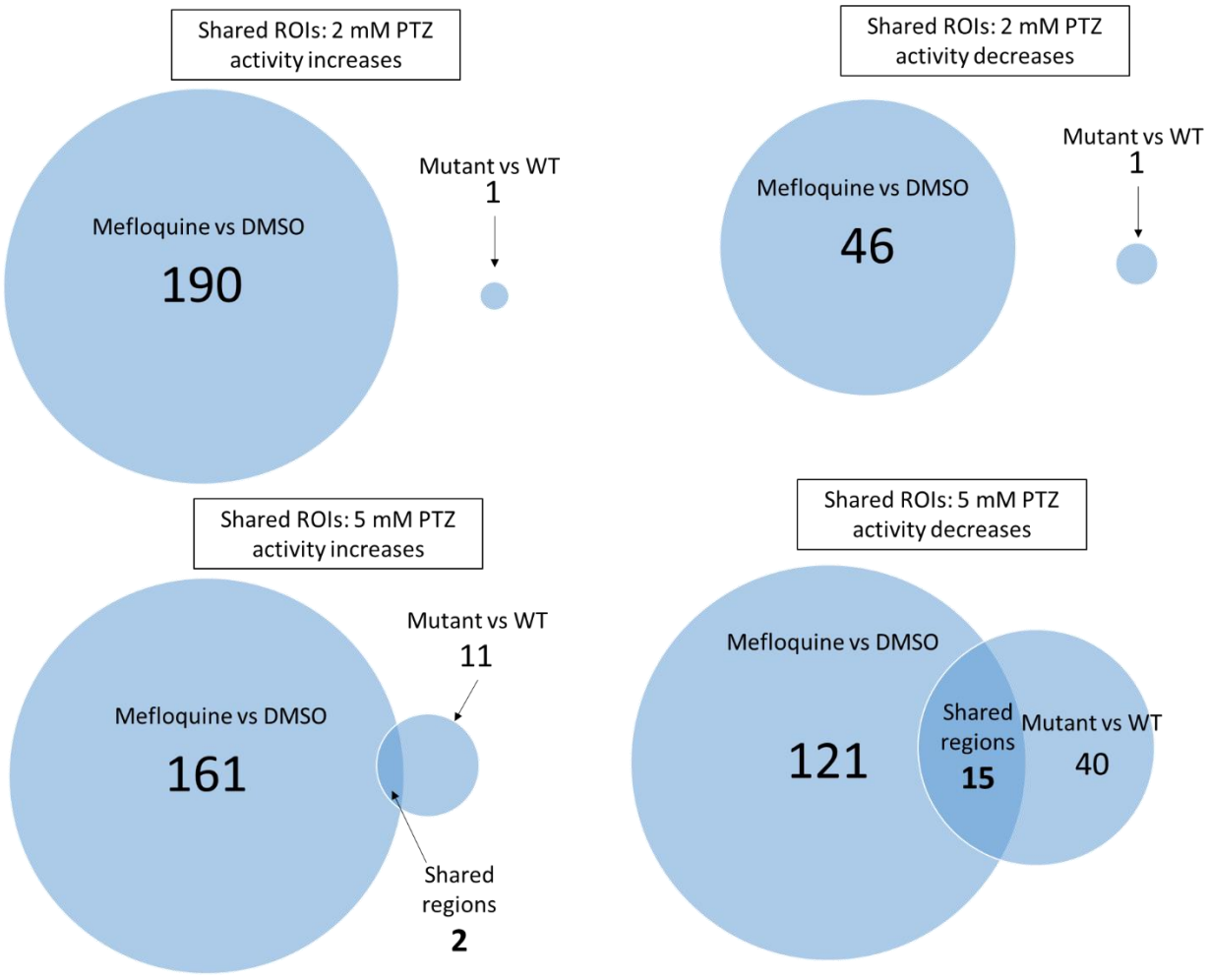
Shared ROIs: 2 mM PTZ activity increases
Mefloquine vs DMSO
190
Mutant vs WT
1
Shared ROIs: 2 mM PTZ activity decreases
Mefloquine vs DMSO
46
Mutant vs WT
1
Shared ROIs: 5 mM PTZ activity increases
Mefloquine vs DMSO
161
Mutant vs WT
11
Shared regions
2
Shared ROIs: 5 mM PTZ activity decreases
Mefloquine vs DMSO
121
Shared regions
15
Mutant vs WT
40

Figure 4.13. Venn diagrams comparing *cx35.5 -/-* and mefloquine vs control significant ROIs (2 and 5 mM PTZ). Depicting comparisons between *cx35.5 -/-* vs control and mefloquine vs control maps for 2 mM PTZ (top) and 5 mM PTZ (bottom) for both increases (left) and decreases (right) in neuronal activity in the given ROI.

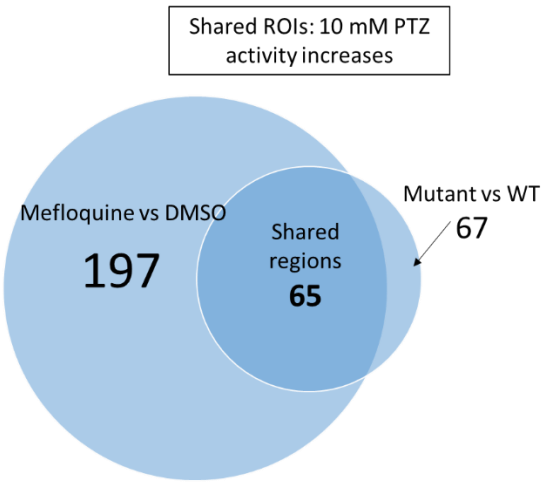
Shared ROIs: 10 mM PTZ activity increases
Mefloquine vs DMSO
197
Shared regions
65
Mutant vs WT
67

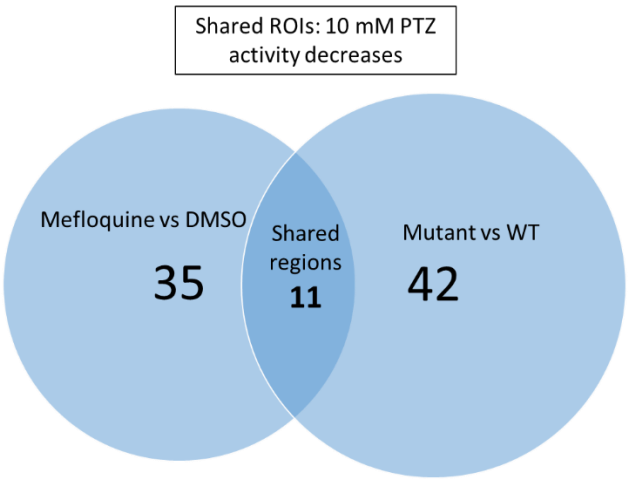
Shared ROIs: 10 mM PTZ activity decreases
Mefloquine vs DMSO
35
Shared regions
11
Mutant vs WT
42

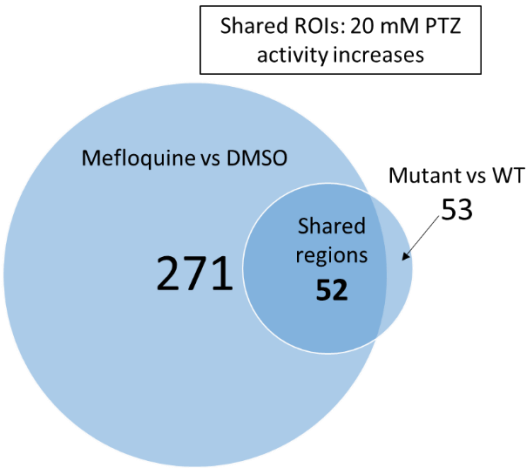
Shared ROIs: 20 mM PTZ activity increases
Mefloquine vs DMSO
271
Shared regions
52
Mutant vs WT
53

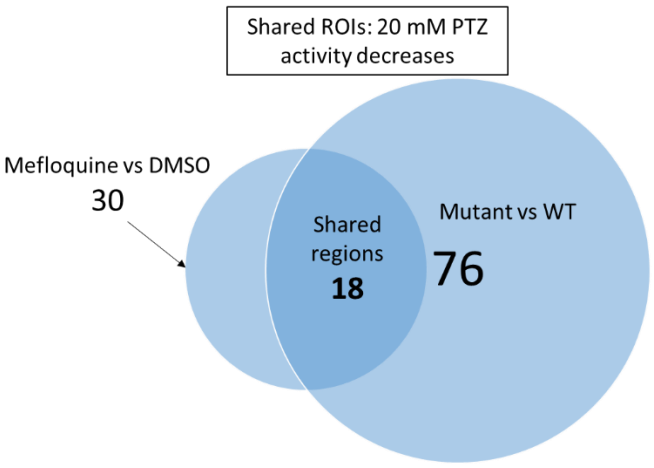
Shared ROIs: 20 mM PTZ activity decreases
Mefloquine vs DMSO
30
Shared regions
18
Mutant vs WT
76

Figure 4.14. Venn Diagrams comparing cx35.5 -/- and mefloquine vs control significant ROIs (10 and 20 mM PTZ). Depicting comparisons between cx35.5 -/- vs control and mefloquine vs control maps for 10 mM PTZ (top) and 20 mM PTZ (bottom) for both increases (left) and decreases (right) in neuronal activity in the given ROI.

4.10 Reduced mefloquine-induced PTZ susceptibility in cx35.5 mutants

The more severe mefloquine phenotype, compared to *c*x35.5 mutants, may be caused by differences in the timing of connexin inhibition. Alternatively, the stronger effects of mefloquine may be caused by more complete inhibition of all Cx36 isoforms or off-target (non-connexin) activity. To distinguish between these possibilities, we examined the effects of mefloquine in *cx35.5-/-* fish. If mefloquine's effects are primarily dependent on Cx35.5 expression, we would expect to see reduced effects of mefloquine in *cx35.5-/-* animals. In contrast, if mefloquine's effects are primarily due to inhibition of other Cx36 isoforms or off-target activity, we would expect to see strong effects of mefloquine in *cx35.5-/-* animals.

We compared the differences in neuronal activity in mefloquine treated and DMSO treated *cx35.5-/-* fish, with 0 (embryo media only), 5, or 20 mM PTZ (Figure 4.15). In all conditions, we observed decreases in neuronal activity within the telencephalon (olfactory bulb, subpallium, pallium), the diencephalon (habenula, retinal arborization fields), and the rhombencephalon (inferior olive). In both the embryo media and 5 mM PTZ conditions, we observed increases in neuronal activity following the administration of mefloquine in a small region of the rhombencephalon (area postrema, neuropil, rhombomere 7) (Figure 4.15B). At 20 mM PTZ, we observe small increases in activity in smaller neuron clusters and observe significant decreases in the telencephalon (olfactory bulb, pallium, subpallium), diencephalon (habenula), and rhombencephalon (Figure 4.15C). These changes in neuronal activity are Cx35.5-independent and are likely off-target effects and may be due to inhibition of other Cx36 isoforms. Nevertheless, the overall effect of mefloquine is greatly reduced in *cx35.5-/-* animals, compared to its effects on wild-type animals (compare Figure 13E-H to Figure 15A-C). Specifically, the pronounced increases in neuronal activity in the hypothalamus, pre-tectum, and subpallium regions were not

seen in the *cx35.5-/-* animals. This result indicates that the main effects of mefloquine are dependent on Cx35.5 expression (Figure 4.15). For a complete list of regions changed, see Supplementary Table 4.

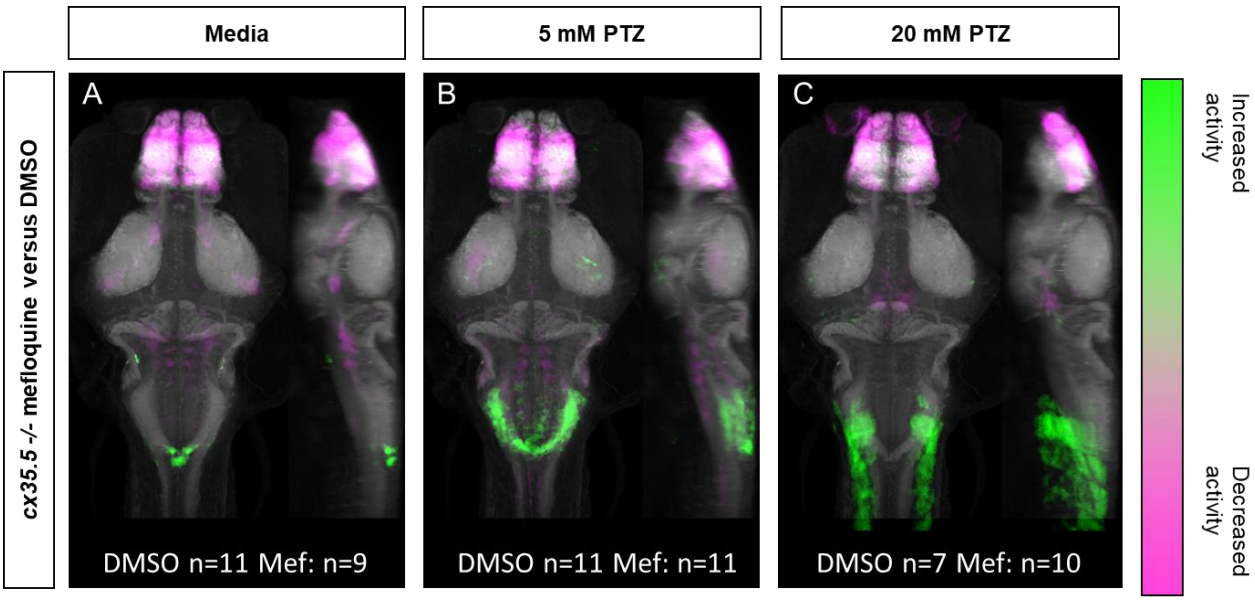
Media
5 mM PTZ
20 mM PTZ
cx35.5 -/- mefloquine versus DMSO
A
B
C
DMSO n=11 Mef: n=9
DMSO n=11 Mef: n=11
DMSO n=7 Mef: n=10
Increased activity
Decreased activity

Figure 4.15. Whole-brain activity map showing off-target effects of mefloquine using cx35.5-/- treated with mefloquine. Dorsal and lateral view of zebrafish larvae brain. Images show pixels with significantly increased pERK/tERK ratio in A) Embryo medium and mefloquine treated compared to DMSO treated larvae. (cx35.5-/- mefloquine n=9, cx35.5-/- DMSO n=11) and B) 5 mM PTZ and mefloquine treated compared to DMSO treated larvae (cx35.5-/- mefloquine n=11 , cx35.5-/- DMSO n=11). C) 20 mM PTZ and mefloquine treated compared to DMSO treated larvae (cx35.5-/- mefloquine n=10 , cx35.5-/- DMSO n=7). For all regions $p < 0.005$

CHAPTER 5: DISCUSSION

5.1 Summary of Findings

The relationship between Cx36 and hyperactivity has been unclear due to the lack of consistent evidence. This due to, in part, inconsistency with methods of inducing seizure, methods for quantifying protein expression, and a lack of brain-wide activity mapping. In this study, we were able to directly compare the reciprocal relationship between Cx36 and hyperactivity through examining whole-brain activity and protein expression in the zebrafish model. We discovered that Cx35.5 mutation results in differential susceptibility to the seizure-inducing drug, PTZ. We observed regional differences in susceptibility with some regions showing increases or decreases in susceptibility to PTZ induced hyperactivity. We also were able to generate a dose-dependent activity map in both wild-type and *cx35.5-/-* fish, indicating significant dose-dependent effects of PTZ. We were able to determine that results were not due to differential cell-death by measure caspase-3 positive cells.

To understand the reciprocal relationship, we created and utilized a whole-brain expression map to examine the expression of Cx36 following exposure to PTZ. We found an acute, immediate decrease in Cx36 expression following exposure to PTZ. This reduction was maintained and then recovered by 3 hours post-PTZ exposure. We were able to confirm that this reduction was not due to increases in cell-death as measured by caspase-3 positive cells.

Finally, to understand if this acute reduction in Cx36 expression we observed caused an increase in susceptibility to PTZ induced hyperactivity, we utilized the Cx36 blocking drug mefloquine. We used mefloquine to acutely block the functionality of the Cx36 channels within the brain, and then observed its effect on whole-brain activity following exposure to PTZ. We

found substantial increases in neuronal hyperactivity following exposure to mefloquine compared to DMSO treated controls at all concentrations of PTZ, indicating an increase in susceptibility to PTZ induced seizures. We confirmed that the majority of this result was not due to off-target effects by treating *cx35.5-/-* fish mefloquine and examining off-target effects on neuronal hyperactivity.

5.2 PTZ exerts brain-wide and region-specific effects

We generated dose-varying whole-brain activity maps for PTZ in *cx35.5-/-* and wild-type fish. Using the zebrafish model we discovered additional regions affected by PTZ that were not examined in previous studies (Baxendale et al. 2012; Baraban et al. 2005; Liu and Baraban 2019; Diaz Verdugo et al. 2019) due to the increased spatial specificity of the MAP-Mapping method (Randlett et al. 2015). This is important because many previous studies in mammalian systems were restricted to the hippocampus. Approximately 3 in 1000 people have temporal lobe epilepsy (TLE) are characterized by hippocampal sclerosis, with 17% of those patients suffering from drug-resistant epilepsy (Asadi-Pooya et al. 2017). In all forms of epilepsy, however, approximately 30% of cases are drug-resistant (Kwan and Brodie 2000). It is therefore imperative to look beyond the hippocampus to address this unmet need.

We did see a slight increase in activity in the pallium at all concentrations of PTZ (analogous to the hippocampus) (Cheng, Jesuthasan, and Penney 2014) (Figure 4.1), but it was not the largest increase we observed. We showed a dose-varying dependent increase in activity after administration of PTZ (Figure 4.1) with larger increases in regions associated with hormone release, and production, as well as executive functioning. These results stress the lack of generalizability of results across brain regions, and the need for expanded inquiry when examining neuronal hyperactivity.

While we were able to examine a greater number of brain regions than previous studies, we sacrificed temporal resolution (achieved with Ca2+ imaging and EEG). However, these results can be used to inform which brain regions should be investigated using methods that allow for greater temporal resolution. In addition to discovering new brain regions affected by PTZ, we were able to better elucidate the dose-varying effects of PTZ. Previous studies, using live calcium imaging, observed increases in neuronal activity and synchronicity after PTZ administration, with differential recruitment of different brain regions (Diaz Verdugo et al. 2019; Liu and Baraban 2019). They observed increases in neuronal activity originating in the pallium and traveling to the hindbrain (Liu and Baraban 2019). Additionally, they observed significant increases in neuronal connectivity in each of the regions observed (Diaz Verdugo et al. 2019). Additionally, previous work in younger zebrafish (2 dpf) found changes in *fos* expression following administration of PTZ in a similar manner (Baxendale et al. 2012). Our results show similar effects of PTZ on brain activity in similar regions, but we were able to identify additional brain regions than was previously possible (Liu and Baraban 2019; Diaz Verdugo et al. 2019; Baxendale et al. 2012). This demonstrates the importance of identifying brain-wide region-specific effects when examining hyperactivity. Taken together, these results illustrate the unique dose-varying whole-brain effects of PTZ that can be expanded upon in future work.

5.3 *cx35.5* knockdown causes region-specific changes in hyperactivity following PTZ administration

In addition to characterizing the effect of PTZ on whole-brain activity in wild-type animals, we gained insight into the drug's effects in *cx35.5-/-* zebrafish. We found neuronal activity differences in *cx35.5-/-* compared to wild-type animals following high concentrations of PTZ (Figure 4.3). We saw increases in regions identified in our PTZ dose-response experiment,

indicating more severe increases in neuronal hyperactivity following the administration of PTZ in those regions (Figure 4.1, Figure 4.3). These results are consistent with previous behavior work by Jacobson, et. al, 2010, which showed that in Cx36 mutant mice, PTZ administration resulted in more severe seizure-associated behaviors than their wild-type counterparts (Jacobson et al. 2010), but also provides more information relating to the severity of neuronal hyperactivity. In addition to activity increases, we observed significant decreases in neuronal activity at 10 mM PTZ concentrations. These decreases were observed in the rhombencephalon, specifically in regions that rely on Cx36 for synchronous firing (inferior olive, Mauthner cells) (Yao et al. 2014; Flores et al. 2012; Bazzigaluppi et al. 2017). These results are important, as it is the first study to show regional differences in neuronal activity between Cx36-deficient and wild-type animals, which indicates the lack of generalizability from region to region within the brain when examining connexin proteins.

5.4 PTZ induced hyperactivity causes a regionally-specific decrease in Cx36 expression

To further understand the relationship between Cx36 and hyperactivity, we asked the reciprocal question: how does hyperactivity affect Cx36? Similar to the seizure susceptibility studies, work to identify this relationship has remained inconclusive (Laura et al. 2015; Motaghi et al. 2017; Söhl et al. 2000; X. Wu et al. 2017). Previous approaches used to address this question (e.g., qPCR, western blot) lacked the necessary spatial resolution to determine if the effects of hyperactivity on Cx36 vary based on the brain region. To address these shortcomings, we developed a novel method for quantifying the whole-brain expression of the Cx36 protein, using antibody staining in conjunction with a modified MAP-mapping technique (Figure 4.5). We were, therefore, able to determine that there are regional and exposure time differences in the

reduction of Cx36 in response to seizure induction using PTZ. Specifically, we saw reductions in a region-specific manner after exposure to PTZ for 30 minutes, and those reductions were greater after 1 hour of PTZ exposure (Figure 4.7). Therefore, we have determined PTZ exerts region-specific effects on Cx36 and that changes found in one region of the brain may not be directly applicable to other regions.

5.5 Reduction in Cx36 expression following hyperactivity is acute and recovers over time

After observing a decrease in Cx36 expression following exposure to PTZ, we measured the temporal patterns of this change. We found that the change in Cx36 expression was acute: it occurred within the first hour of PTZ exposure and was almost fully recovered by 3 hours (Figure 4.8A, B). The recovery was then slightly overshot, Cx36 was overexpressed in the optic tectum and cerebellum as well as other brain regions, and this overexpression was maintained 24 hours later (Figure 4.8C, D). Because the reduction was not caused by an increase in cell death (Figure 4.9), this effect is likely due to an increase in endocytosis and degradation of the Cx36 protein. Various studies have shown that activity-dependent modulation of Cx36 proteins exists (Smith and Pereda 2003; Haas, Greenwald, and Pereda 2016) and due to the fast decrease of Cx36 expression, endocytosis is a likely mechanism by which this can occur (Flores et al. 2012). Considering the longer-term recovery (3 hours) and then overshoot of expression (6 hours and 24 hours later) it is also likely that a change in transcription is also occurring. Production of Cx36 is likely either slowed or halted and then increased to recover the protein. This process lags behind total protein production, which is why overshoot is observed.

5.6 Acute reduction in Cx36 functionality leaves organisms more susceptible to PTZ induced hyperactivity

To solidify the relationship between hyperactivity and Cx36, we studied how acute blockade of Cx36 affects susceptibility to hyperactivity. Is the reduction in Cx36 after PTZ exposure adaptive, maladaptive, or inconsequential? To answer this question, we utilized the Cx36 specific blocking drug mefloquine and expose mefloquine treated and untreated fish to PTZ. Mefloquine is an anti-malarial drug that selectively blocks Cx36 and Cx50. Previous studies utilized quinine which has more off-target effects. It is hypothesized that mefloquine blocks Cx36 by binding to the inside of the pore, preventing the flow of ions through that pore (Harris and Locke 2008). We found a significant increase in neuronal hyperactivity following treatment with PTZ in the mefloquine treated fish compared to control (Figure 4.12). This result indicates a reduction in Cx36 in all cases (acute and chronic) is detrimental and leads to an altered severity of hyperactivity.

At moderate doses (6-25 µM), mefloquine can exhibit off-target effects of varying degrees (Caridha et al. 2008; McArdle et al. 2006; Harris and Locke 2008). To better understand the non-Cx36 effects of mefloquine, we treated *cx35.5-/-* fish with mefloquine and quantified changes in neuronal activity both at rest (in embryo medium) and after PTZ (5 mM). We observed major decreases in neuronal activity within the forebrain and a slight decrease in the rhombencephalon in both conditions. Additionally, we observed a slight increase in neuronal activity in the rhombencephalon which was exacerbated slightly by PTZ (Figure 4.12). We attribute these effects to the off-target effects of mefloquine. As such, in wild-type animals, changes we observed in PTZ sensitivity in other regions are more likely to be caused by Cx36 blockade.

We found that the effects of mefloquine on PTZ-induced neuronal hyperactivity (Figure 4.12) were greater than that of the *cx35.5* knockout (Figure 4.3, Figure 4.13, Figure 4.14). This may be due to the difference between acute (mefloquine) versus congenital (*cx35.5*) perturbation in overall Cx36 function. In the *cx35.5* mutants, there may be compensatory mechanisms that can partially ameliorate the effects of reduced Cx36 function (Rossi et al. 2015). Additionally, it is important to note that while overall Cx36 levels (as measured by Cx36 immunolabeling) is significantly reduced in *cx35.5-/-* animals, there is still some residual Cx34.1 expression. Thus, the more severe phenotype seen in the mefloquine treated animals may reflect a more complete inhibition of all Cx36 isoforms. Finally, while we selected mefloquine due to its selective activity towards Cx36, it does still exert off-target effects, including blockage of other connexin proteins and may be toxic (Cruikshank et al. 2004). Nevertheless, the main effect of mefloquine on PTZ-induced hyperactivity depends on Cx35.5 expression (Figure 4.15), which supports our interpretation that acute knockdown of zebrafish Cx36 proteins by mefloquine results in increased susceptibility to neuronal hyperactivity (Figure 4.12).

5.7 Cx36 is a contributing factor regulating the brains response to hyperactivity

A plausible relationship to human disease is in Juvenile Myoclonic Epilepsy (JME). Individuals with JME have a higher likelihood of harboring a specific intronic SNP in the *Cx36* gene (Mas et al. 2004; Hempelmann, Heils, and Sander 2006). This SNP has been hypothesized to affect splicing enhancers of the gene, therefore affecting the translation of the protein (Mas et al. 2004). While Cx36 is not the only cause for diseases like JME, it may be a contributing factor. Based on our results, loss of Cx36 would be predicted to make an individual more susceptible to other factors leading to hyperactivity, increasing the severity of hyperactivity (Figure 1, 6), This

is particularly relevant as Cx36 expression is highest during development and decreases over time (Belousov and Fontes 2013) and JME first appears in children and adolescents.

Our work demonstrates that Cx36 appears to reduce PTZ induced hyperactivity in specific brain regions and that loss of the protein is detrimental to that process. We were able to determine where in the brain we see effects in addition to when those changes occur. This work provides a basis for better understanding the role of Cx36 and PTZ induced hyperactivity.

5.8 Future Directions

While we were able to discern many aspects of the relationship between Cx36 and hyperactivity, there is still more work to be done to fully understand this interaction. We were able to determine that exposure to the seizure-inducing drug PTZ lead to a decrease in Cx36 expression over time. Going forward, we will need to attempt to determine what is causing this change to occur. This increase could be due to either an increase in endocytosis, a decrease in production and implantation of the protein, or a combination of both. To test this, future studies should examine the transcript levels of Cx36 either through in situ hybridization, to maintain the spatial information, and determine if changes in transcription occur after exposure to PTZ. To test if changes in endocytosis exist, ideally, blockade of Cx36 specific endocytosis would be done. Drugs currently exist for Cx43 and specifically blocks the endocytosis of Cx43, however, this kind of drug does not exist for Cx36. Alternatively, one could perform co-immunoprecipitation to examine quantities of conjugated Cx36 with endocytosis markers such as dynamin-2 to determine changes in endocytosis, specifically, over time.

In addition to changes in expression, changes in the functionality of the protein (conductance of the pore) could exist. Previous work has shown that changes in activity and calcium affect the functionality of the connexin pore (Wang and Belousov 2011; Haas, Zavala,

and Landisman 2011). As such, it is important to also examine changes in the functionality of the Cx36 pore following exposure to PTZ. To do this, one could perform a dye tracing experiment in which a dye is injected into a cell known to be coupled to another cell through a gap junction, and the transfer of that dye into the known couped cell to determine if changes in functionality of the pore exist.

We observed regional and dose-dependent changes in neuronal hyperactivity following exposure to PTZ in both mutant (*cx35.5-/-)* and animals treated with the Cx36 blocking drug mefloquine. The impact of these regional differences, however, still needs to be explored. We know that Cx36 coupled cells in regions such as the inferior olive and cerebellum are mainly between inhibitory interneurons (Bazzigaluppi et al. 2017), while regions such as the cerebellum, specifically the Golgi cells, are mainly coupled between excitatory neurons (Vervaeke et al. 2010). The regional changes in sensitivity may be due to differences in cell-type coupling. To test this, one could create a cell-type-specific (excitatory and inhibitory neurons) and a regional dependent knock-out using tissue-specific CRISPR knock-out (Yin et al. 2015) of Cx36 to determine if one cell-type or specific region(s) contribute more or less to this effect.

While the zebrafish provides a unique experimental system that has many benefits and tools available, it is important to replicate these results in other animal models, and specifically within mammals. We were able to replicate similar findings to those in rats and mice showing that PTZ exhibits regions specific effects on brain activity in wild-type animals (Yang et al. 2019; Barros et al. 2015; Nehlig 1998) and these experiments should be replicated using Cx36-knockout and mefloquine treated animals. Additionally, whole-brain changes in Cx36 expression should also be examined in mammalian systems. If replicated, these results will strengthen the likelihood that Cx36 is a viable therapeutic target.

Finally, we used only one method of seizure induction, PTZ. Many other forms of seizure induction exist and should be tested. PTZ acts through inhibition of GABA receptors, therefore reducing the amount of inhibition and increasing excitation. Other methods of seizure induction, such as kainic acid, enhance the activity of glutamate (increasing excitation) but not affecting GABA production or function, affect ion channels (4-AP), or affect acetylcholine (pilocarpine) (Kandratavicius, Alves Balista, et al. 2014b). It is therefore important to determine if the changes we observed are specific to seizure induction using PTZ, or if they are specific to seizure activity.

CHAPTER 6: SUMMARY

The goal of this study was to understand the reciprocal relationship between Cx36 and neuronal hyperactivity on a brain-wide scale. We utilized MAP-mapping to quantify neuronal activity and protein expression across the *whole-brain*, which has not been possible using other models. Through this, we characterized the complex nature of this relationship and its dependence on many factors including brain region, drug dose, and exposure time. We found that chronic deficiency of the Cx36 protein in the *cx35.5* mutants altered susceptibility to PTZ-induced neuronal hyperactivity in a region-specific manner. We also developed a whole-brain quantification method for Cx36 expression and found that PTZ exposure results in an acute decrease in the expression of Cx36, followed by recovery and overexpression of the protein. Finally, we observed that acute knockdown of the functionality of Cx36 by mefloquine resulted in a broad increase in the susceptibility to PTZ induced hyperactivity. Taken together, these results suggest that Cx36 acts to prevent hyperactivity within the brain, and that loss of Cx36 protein, both acute (perhaps due to previous hyperactivity) and chronic, results in an increase in susceptibility to hyperactivity.

REFERENCES

Allen, Kevin, Elke C. Fuchs, Hannah Jaschonek, David M. Bannerman, and Hannah Monyer. 2011. “Gap Junctions between Interneurons Are Required for Normal Spatial Coding in the Hippocampus and Short-Term Spatial Memory.” *Journal of Neuroscience* 31 (17): 6542–52. https://doi.org/10.1523/JNEUROSCI.6512-10.2011.

Annegers, J F, W A Hauser, J R Lee, and W A Rocca. 1995. “Incidence of Acute Symptomatic Seizures in Rochester, Minnesota, 1935-1984.” *Epilepsia* 36 (4): 327–33. http://www.ncbi.nlm.nih.gov/pubmed/7607110.

Asadi-Pooya, Ali A., Gregory R. Stewart, Daniel J. Abrams, and Ashwini Sharan. 2017. “Prevalence and Incidence of Drug-Resistant Mesial Temporal Lobe Epilepsy in the United States.” *World Neurosurgery*. Elsevier Inc. https://doi.org/10.1016/j.wneu.2016.12.074.

Baraban, Scott C., Matthew T. Dinday, and Gabriela A. Hortopan. 2013. “Drug Screening in Scn1a Zebrafish Mutant Identifies Clemizole as a Potential Dravet Syndrome Treatment.” *Nature Communications* 4 (1): 2410. https://doi.org/10.1038/ncomms3410.

Baraban, Scott C., M.R. Taylor, P.A. Castro, and H. Baier. 2005. “Pentylenetetrazole Induced Changes in Zebrafish Behavior, Neural Activity and c-Fos Expression.” *Neuroscience* 131 (3): 759–68. https://doi.org/10.1016/J.NEUROSCIENCE.2004.11.031.

Barros, Vanessa N., Mayara Mundim, Layla Testa Galindo, Simone Bittencourt, Marimelia Porcionatto, and Luiz E. Mello. 2015. “The Pattern of C-Fos Expression and Its Refractory Period in the Brain of Rats and Monkeys.” *Frontiers in Cellular Neuroscience* 9 (March): 72. https://doi.org/10.3389/fncel.2015.00072.

Baxendale, Sarah, Celia J. Holdsworth, Paola L. Meza Santoscoy, Michael R.M. Harrison, James Fox, Caroline A. Parkin, Philip W. Ingham, and Vincent T. Cunliffe. 2012. "Identification of Compounds with Anti-Convulsant Properties in a Zebrafish Model of Epileptic Seizures." *DMM Disease Models and Mechanisms* 5 (6): 773–84. https://doi.org/10.1242/dmm.010090.

Bazzigaluppi, Paolo, Sheena C. Isenia, Elize D. Haasdijk, Ype Elgersma, Chris I. De Zeeuw, Ruben S. van der Giessen, and Marcel T. G. de Jeu. 2017. "Modulation of Murine Olivary Connexin 36 Gap Junctions by PKA and CaMKII." *Frontiers in Cellular Neuroscience* 11 (December): 397. https://doi.org/10.3389/fncel.2017.00397.

Belousov, Andrei B., Hiroshi Nishimune, Janna V. Denisova, and Joseph D. Fontes. 2018. "A Potential Role for Neuronal Connexin 36 in the Pathogenesis of Amyotrophic Lateral Sclerosis." *Neuroscience Letters* 666 (February): 1–4. https://doi.org/10.1016/j.neulet.2017.12.027.

Belousov, Andrei B, and Joseph D Fontes. 2013. "Neuronal Gap Junctions: Making and Breaking Connections during Development and Injury." *Trends in Neurosciences* 36 (4): 227–36. https://doi.org/10.1016/j.tins.2012.11.001.

Bender, Alex C., Richard P. Morse, Rod C. Scott, Gregory L. Holmes, and Pierre Pascal Lenck-Santini. 2012. "SCN1A Mutations in Dravet Syndrome: Impact of Interneuron Dysfunction on Neural Networks and Cognitive Outcome." *Epilepsy and Behavior*. NIH Public Access. https://doi.org/10.1016/j.yebeh.2011.11.022.

Cancedda, Laura, Elena Putignano, Soren Impey, Lamberto Maffei, Gian Michele Ratto, and Tommaso Pizzorusso. 2003. "Patterned Vision Causes CRE-Mediated Gene Expression in

the Visual Cortex through PKA and ERK." *Journal of Neuroscience* 23 (18): 7012–20. https://doi.org/10.1523/jneurosci.23-18-07012.2003.

Caridha, D, D Yourick, M Cabezas, L Wolf, T H Hudson, and G S Dow. 2008. "Mefloquine-Induced Disruption of Calcium Homeostasis in Mammalian Cells Is Similar to That Induced by Ionomycin Downloaded From." *ANTIMICROBIAL AGENTS AND CHEMOTHERAPY* 52 (2): 684–93. https://doi.org/10.1128/AAC.00874-07.

Cheng, Ruey Kuang, Suresh J. Jesuthasan, and Trevor B. Penney. 2014. "Zebrafish Forebrain and Temporal Conditioning." *Philosophical Transactions of the Royal Society B: Biological Sciences*. The Royal Society. https://doi.org/10.1098/rstb.2012.0462.

Cho, Sung Joon, Donghak Byun, Tai Seung Nam, Seok Yong Choi, Byung Geun Lee, Myeong Kyu Kim, and Sohee Kim. 2017. "Zebrafish as an Animal Model in Epilepsy Studies with Multichannel EEG Recordings." *Scientific Reports* 7 (1): 1–10. https://doi.org/10.1038/s41598-017-03482-6.

Collignon, Frederic, Nicholas M. Wetjen, Aaron A. Cohen-Gadol, Gregory D. Cascino, Joseph Parisi, Fredric B. Meyer, W. Richard Marsh, Patrick Roche, and Stephen D. Weigand. 2006. "Altered Expression of Connexin Subtypes in Mesial Temporal Lobe Epilepsy in Humans." *Journal of Neurosurgery* 105 (1): 77–87. https://doi.org/10.3171/jns.2006.105.1.77.

Condorelli, Daniele F., Angela Trovato-Salinaro, Giuseppa Mudo, Melita B. Mirone, and Natale Belluardo. 2003. "Cellular Expression of Connexins in the Rat Brain: Neuronal Localization, Effects of Kainate-Induced Seizures and Expression in Apoptotic Neuronal Cells." *European Journal of Neuroscience* 18 (7): 1807–27. https://doi.org/10.1046/j.1460-9568.2003.02910.x.

Cotrina, M. L., J. H.C. Lin, A. Alves-Rodrigues, S. Liu, J. Li, H. Azmi-Ghadimi, J. Kang, C. C.G. Naus, and M. Nedergaard. 1998. “Connexins Regulate Calcium Signaling by Controlling ATP Release.” *Proceedings of the National Academy of Sciences of the United States of America* 95 (26): 15735–40. https://doi.org/10.1073/pnas.95.26.15735.

Cruikshank, Scott J, Matthew Hopperstad, Meg Younger, Barry W Connors, David C Spray, and Miduturu Srinivas. 2004. “Potent Block of Cx36 and Cx50 Gap Junction Channels by Mefloquine.” www.pnas.orgcgidoi10.1073pnas.0402044101.

Dai, Yi, Koichi Iwata, Tetsuo Fukuoka, Eiji Kondo, Atsushi Tokunaga, Hiroki Yamanaka, Toshiya Tachibana, Yi Liu, and Koichi Noguchi. 2002. “Phosphorylation of Extracellular Signal-Regulated Kinase in Primary Afferent Neurons by Noxious Stimuli and Its Involvement in Peripheral Sensitization.” *Journal of Neuroscience* 22 (17): 7737–45. https://doi.org/10.1523/jneurosci.22-17-07737.2002.

Davies, J A. 1995. “Mechanisms of Action of Antiepileptic Drugs.” *Seizure* 4 (4): 267–71. http://www.ncbi.nlm.nih.gov/pubmed/8719918.

Diaz Verdugo, Carmen, Sverre Myren-Svelstad, Ecem Aydin, Evelien Van Hoeymissen, Celine Deneubourg, Silke Vanderhaeghe, Julie Vancraeynest, et al. 2019. “Glia-Neuron Interactions Underlie State Transitions to Generalized Seizures.” *Nature Communications* 10 (1): 1–13. https://doi.org/10.1038/s41467-019-11739-z.

Dobrenis, Konstantin, H. Y. Chang, M. H. Pina-Benabou, A. Woodroffe, S. C. Lee, R. Rozental, D. C. Spray, and E. Scemes. 2005. “Human and Mouse Microglia Express Connexin36, and Functional Gap Junctions Are Formed between Rodent Microglia and Neurons.” *Journal of Neuroscience Research* 82 (3): 306–15. https://doi.org/10.1002/jnr.20650.

Dravet, Charlotte. 2011. “The Core Dravet Syndrome Phenotype.” *Epilepsia* 52 (April): 3–9. https://doi.org/10.1111/j.1528-1167.2011.02994.x.

Ezan, Pascal, Pascal André, Salvatore Cisternino, Bruno Saubaméa, Anne Cécile Boulay, Suzette Doutremer, Marie Annick Thomas, Nicole Quenech’Du, Christian Giaume, and Martine Cohen-Salmon. 2012. “Deletion of Astroglial Connexins Weakens the Blood-Brain Barrier.” *Journal of Cerebral Blood Flow and Metabolism* 32 (8): 1457–67. https://doi.org/10.1038/jcbfm.2012.45.

Flores, C. E., S. Nannapaneni, K. G. V. Davidson, T. Yasumura, M. V. L. Bennett, J. E. Rash, and A. E. Pereda. 2012. “Trafficking of Gap Junction Channels at a Vertebrate Electrical Synapse in Vivo.” *Proceedings of the National Academy of Sciences* 109 (9): E573–82. https://doi.org/10.1073/pnas.1121557109.

Gajda, Zita, Zoltán Szupera, Gábor Blazsó, and Magdolna Szente. 2005. “Quinine, a Blocker of Neuronal Cx36 Channels, Suppresses Seizure Activity in Rat Neocortex In Vivo.” *Epilepsia* 46 (10): 1581–91. https://s3.amazonaws.com/objects.readcube.com/articles/downloaded/wiley/94cebc1e11a9dc9bdbfd8c0e7826390905ed9531776beba8cff9957776fd8406.pdf?X-Amz-Algorithm=AWS4-HMAC-SHA256&X-Amz-Credential=AKIAIS5LBPCM5JPOCDGQ%2F20180319%2Fus-east-1%2Fs3%2Faws4_request&.

Garbelli, R., C. Frassoni, D. F. Condorelli, A. Trovato Salinaro, N. Musso, V. Medici, L. Tassi, M. Bentivoglio, and R. Spreafico. 2011. “Expression of Connexin 43 in the Human Epileptic and Drug-Resistant Cerebral Cortex.” *Neurology* 76 (10): 895–902.

https://doi.org/10.1212/WNL.0b013e31820f2da6.

Giaume, Christian, and Christian C Naus. 2013. “Connexins, Gap Junctions, and Glia.” *WIREs Membr Transp Signal* 2: 133–42. https://doi.org/10.1002/wmts.87.

Haas, Julie S., Corey M. Greenwald, and Alberto E. Pereda. 2016. “Activity-Dependent Plasticity of Electrical Synapses: Increasing Evidence for Its Presence and Functional Roles in the Mammalian Brain.” *BMC Cell Biology* 17 (S1): 14. https://doi.org/10.1186/s12860-016-0090-z.

Haas, Julie S, Baltazar Zavala, and Carole E Landisman. 2011. “Activity-Dependent Long-Term Depression of Electrical Synapses.” *Science (New York, N.Y.)* 334 (6054): 389–93. https://doi.org/10.1126/science.1207502.

Harris, Andrew, and Darren Locke, eds. 2008. *Connexins: A Guide*. Illustrate. New York, NY: Springer Science & Business Media.

Hauser, W A, J F Annegers, and L T Kurland. n.d. “Incidence of Epilepsy and Unprovoked Seizures in Rochester, Minnesota: 1935-1984.” *Epilepsia* 34 (3): 453–68. Accessed June 21, 2018. http://www.ncbi.nlm.nih.gov/pubmed/8504780.

Hempelmann, Anne, Armin Heils, and Thomas Sander. 2006. “Confirmatory Evidence for an Association of the Connexin-36 Gene with Juvenile Myoclonic Epilepsy.” *Epilepsy Research* 71 (2–3): 223–28. https://doi.org/10.1016/J.EPLEPSYRES.2006.06.021.

Hestrin, Shaul, and Mario Galarreta. 2005. “Electrical Synapses Define Networks of Neocortical GABAergic Neurons.” *Trends in Neurosciences* 28 (6): 304–9. https://doi.org/10.1016/j.tins.2005.04.001.

Howe, Kerstin, Matthew D. Clark, Carlos F. Torroja, James Torrance, Camille Berthelot, Matthieu Muffato, John E. Collins, et al. 2013. “The Zebrafish Reference Genome Sequence and Its Relationship to the Human Genome.” *Nature* 496 (7446): 498–503. https://doi.org/10.1038/nature12111.

Jacobson, Gregory M., Logan J. Voss, Sofia M. Melin, Jonathan P. Mason, Ray T. Cursons, D. Alistair Steyn-Ross, Moira L. Steyn-Ross, and James W. Sleigh. 2010. “Connexin36 Knockout Mice Display Increased Sensitivity to Pentylenetetrazol-Induced Seizure-like Behaviors.” *Brain Research* 1360 (November): 198–204. https://doi.org/10.1016/J.BRAINRES.2010.09.006.

Ji, Ru Rong, Hiroshi Baba, Gary J. Brenner, and Clifford J. Woolf. 1999. “Nociceptive-Specific Activation of ERK in Spinal Neurons Contributes to Pain Hypersensitivity.” *Nature Neuroscience* 2 (12): 1114–19. https://doi.org/10.1038/16040.

Kandratavicius, Ludmyla, Priscila Alves Balista, Cleiton Lopes-Aguiar, Rafael Naime Ruggiero, Eduardo Henrique Umeoka, Norberto Garcia-Cairasco, Lezio Soares Bueno-Junior, and Joao Pereira Leite. 2014a. “Animal Models of Epilepsy: Use and Limitations.” *Neuropsychiatric Disease and Treatment*. Dove Medical Press Ltd. https://doi.org/10.2147/NDT.S50371.

———. 2014b. “Animal Models of Epilepsy: Use and Limitations.” *Neuropsychiatric Disease and Treatment*. Dove Medical Press Ltd. https://doi.org/10.2147/NDT.S50371.

Kandratavicius, Ludmyla, Priscila Alves Balista, Cleiton Lopes-Aguiar, Rafael Naime Ruggiero, Eduardo Henrique Umeoka, Norberto Garcia-Cairasco, Lezio Soares Bueno-Junior, and Joao Pereira Leite. 2014. “Animal Models of Epilepsy: Use and Limitations.”

Neuropsychiatric Disease and Treatment 10: 1693–1705. https://doi.org/10.2147/NDT.S50371.

Kofuji, P., and E. A. Newman. 2004. "Potassium Buffering in the Central Nervous System." *Neuroscience* 129 (4): 1043–54. https://doi.org/10.1016/j.neuroscience.2004.06.008.

Kovács-Öller, Tamás, Gábor Debertin, Márton Balogh, Alma Ganczer, József Orbán, Miklós Nyitrai, Lajos Balogh, Orsolya Kántor, and Béla Völgyi. 2017. "Connexin36 Expression in the Mammalian Retina: A Multiple-Species Comparison." *Frontiers in Cellular Neuroscience* 11 (March): 65. https://doi.org/10.3389/fncel.2017.00065.

Krumholz, A, G Y Sung, R S Fisher, E Barry, G K Bergey, and L M Grattan. 1995. "Complex Partial Status Epilepticus Accompanied by Serious Morbidity and Mortality." *Neurology* 45 (8): 1499–1504. https://doi.org/10.1212/WNL.45.8.1499.

Kwan, Patrick, and Martin J. Brodie. 2000. "Early Identification of Refractory Epilepsy." *New England Journal of Medicine* 342 (5): 314–19. https://doi.org/10.1056/NEJM200002033420503.

Laird, Dale W. 2006. "Life Cycle of Connexins in Health and Disease." *Biochemical Journal*. Portland Press Ltd. https://doi.org/10.1042/BJ20051922.

Laura, Medina-Ceja, Flores-Ponce Xóchitl, Santerre Anne, and Morales-Villagrán Alberto. 2015. "Analysis of Connexin Expression during Seizures Induced by 4-Aminopyridine in the Rat Hippocampus." *Journal of Biomedical Science* 22 (1): 69. https://doi.org/10.1186/s12929-015-0176-5.

Liu, Jing, and Scott C. Baraban. 2019. "Network Properties Revealed during Multi-Scale

Calcium Imaging of Seizure Activity in Zebrafish." *Eneuro* 6 (1): ENEURO.0041-19.2019. https://doi.org/10.1523/ENEURO.0041-19.2019.

Lu, Chengbiao, and Mark P. Mattson. 2001. "Dimethyl Sulfoxide Suppresses NMDA- and AMPA-Induced Ion Currents and Calcium Influx and Protects against Excitotoxic Death in Hippocampal Neurons." *Experimental Neurology* 170 (1): 180–85. https://doi.org/10.1006/exnr.2001.7686.

Maack, G., and H. Segner. 2003. "Morphological Development of the Gonads in Zebrafish." *Journal of Fish Biology* 62 (4): 895–906. https://doi.org/10.1046/j.1095-8649.2003.00074.x.

Manjarrez-Marmolejo, Joaquín, and Javier Franco-Pérez. 2016. "Gap Junction Blockers: An Overview of Their Effects on Induced Seizures in Animal Models." *Current Neuropharmacology* 14 (7): 759–71. https://doi.org/10.2174/1570159x14666160603115942.

Marsh, Audrey J., Jennifer Carlisle Michel, Anisha P. Adke, Emily L. Heckman, and Adam C. Miller. 2017. "Asymmetry of an Intracellular Scaffold at Vertebrate Electrical Synapses." *Current Biology* 27 (22): 3561-3567.e4. https://doi.org/10.1016/J.CUB.2017.10.011.

Mas, C, N Taske, S Deutsch, M Guipponi, P Thomas, A Covanis, M Friis, et al. 2004. "Association of the Connexin36 Gene with Juvenile Myoclonic Epilepsy." *J Med Genet* 41. https://doi.org/10.1136/jmg.2003.017954.

McArdle, Joseph J., Lawrence C. Sellin, Kathleen M. Coakley, Joseph G. Potian, and Kormakur Hognason. 2006. "Mefloquine Selectively Increases Asynchronous Acetylcholine Release from Motor Nerve Terminals." *Neuropharmacology* 50 (3): 345–53.

https://doi.org/10.1016/j.neuropharm.2005.09.011.

Miller, Adam C, Alex C Whitebirch, Arish N Shah, Kurt C Marsden, Michael Granato, John O'Brien, and Cecilia B Moens. 2017. "A Genetic Basis for Molecular Asymmetry at Vertebrate Electrical Synapses." *ELife* 6 (May). https://doi.org/10.7554/eLife.25364.

Mills, Stephen L., Jennifer J. O'Brien, Wei Li, John O'Brien, and Stephen C. Massey. 2001. "Rod Pathways in the Mammalian Retina Use Connexin 36." *Journal of Comparative Neurology* 436 (3): 336–50. https://doi.org/10.1002/cne.1071.

Morgan, Victoria L., John C. Gore, and Bassel Abou-Khalil. 2010. "Functional Epileptic Network in Left Mesial Temporal Lobe Epilepsy Detected Using Resting FMRI." *Epilepsy Research* 88 (2–3): 168–78. https://doi.org/10.1016/j.eplepsyres.2009.10.018.

Motaghi, Sahel, Mohammad Sayyah, Vahab Babapour, and Reza Mahdian. 2017. "Hippocampal Expression of Connexin36 and Connexin43 during Epileptogenesis in Pilocarpine Model of Epilepsy." *Iranian Biomedical Journal* 21 (3): 167–73. https://doi.org/10.18869/ACADPUB.IBJ.21.3.167.

Nehlig, Astrid. 1998. "Mapping of Neuronal Networks Underlying Generalized Seizures Induced by Increasing Doses of Pentylenetetrazol in the Immature and Adult Rat: A c-Fos Immunohistochemical Study." *European Journal of Neuroscience* 10 (6): 2094–2106. https://doi.org/10.1046/j.1460-9568.1998.00223.x.

Purves, Dale, George J Augustine, David Fitzpatrick, Lawrence C Katz, Anthony-Samuel LaMantia, James O McNamara, and S Mark Williams. 2001. "Electrical Synapses." https://www.ncbi.nlm.nih.gov/books/NBK11164/.

Randlett, Owen, Caroline L Wee, Eva A Naumann, Onyeka Nnaemeka, David Schoppik, James E Fitzgerald, Ruben Portugues, et al. 2015. “Whole-Brain Activity Mapping onto a Zebrafish Brain Atlas.” *Nature Methods* 12 (11): 1039–46. https://doi.org/10.1038/nmeth.3581.

Rash, John E., Naomi Kamasawa, Kimberly G. V. Davidson, Thomas Yasumura, Alberto E. Pereda, and James I. Nagy. 2012. “Connexin Composition in Apposed Gap Junction Hemiplaques Revealed by Matched Double-Replica Freeze-Fracture Replica Immunogold Labeling.” *The Journal of Membrane Biology* 245 (5–6): 333–44. https://doi.org/10.1007/s00232-012-9454-2.

Retamal, Mauricio A., Nicolas Froger, Nicolas Palacios-Prado, Pascal Ezan, Pablo J. Sáez, Juan C. Sáez, and Christian Giaume. 2007. “Cx43 Hemichannels and Gap Junction Channels in Astrocytes Are Regulated Oppositely by Proinflammatory Cytokines Released from Activated Microglia.” *Journal of Neuroscience* 27 (50): 13781–92. https://doi.org/10.1523/JNEUROSCI.2042-07.2007.

Rossi, Andrea, Zacharias Kontarakis, Claudia Gerri, Hendrik Nolte, Soraya Hölper, Marcus Krüger, and Didier Y.R. Stainier. 2015. “Genetic Compensation Induced by Deleterious Mutations but Not Gene Knockdowns.” *Nature* 524 (7564): 230–33. https://doi.org/10.1038/nature14580.

Schulz, Rainer, Philipp Maximilian Görge, Anikó Görbe, Péter Ferdinandy, Paul D. Lampe, and Luc Leybaert. 2015. “Connexin 43 Is an Emerging Therapeutic Target in Ischemia/Reperfusion Injury, Cardioprotection and Neuroprotection.” *Pharmacology and Therapeutics*. Elsevier Inc. https://doi.org/10.1016/j.pharmthera.2015.06.005.

Shah, Arish N., Crystal F. Davey, Alex C. Whitebirch, Adam C. Miller, and Cecilia B. Moens. 2015. “Rapid Reverse Genetic Screening Using CRISPR in Zebrafish.” *Nature Methods* 12 (6): 535–40. https://doi.org/10.1038/nmeth.3360.

Shandra, Oleksii, Alexander R. Winemiller, Benjamin P. Heithoff, Carmen Munoz-Ballester, Kijana K. George, Michael J. Benko, Ivan A. Zuidhoek, et al. 2019. “Repetitive Diffuse Mild Traumatic Brain Injury Causes an Atypical Astrocyte Response and Spontaneous Recurrent Seizures.” *Journal of Neuroscience* 39 (10): 1944–63. https://doi.org/10.1523/JNEUROSCI.1067-18.2018.

Shehab, Safa, Peter Coffey, Paul Dean, and Peter Redgrave. 1992. “Regional Expression of Fos-like Immunoreactivity Following Seizures Induced by Pentylenetetrazole and Maximal Electroshock.” *Experimental Neurology* 118 (3): 261–74. https://doi.org/10.1016/0014-4886(92)90183-Q.

Shin, Samuel I. 2013. “Connexin-36 Knock-Out Mice Have Increased Threshold for Kindled Seizures: Role of GABA Inhibition.” *Biochemistry & Pharmacology: Open Access* S (1). https://doi.org/10.4172/2167-0501.S1-006.

Smith, Mackenzie, and Alberto E Pereda. 2003. “Chemical Synaptic Activity Modulates Nearby Electrical Synapses.” *Proceedings of the National Academy of Sciences of the United States of America* 100 (8): 4849–54. https://doi.org/10.1073/pnas.0734299100.

Söhl, Goran, Martin Güldenagel, Heinz Beck, Barbara Teubner, Otto Traub, Rafael Gutiérrez, Uwe Heinemann, and Klaus Willecke. 2000. “Expression of Connexin Genes in Hippocampus of Kainate-Treated and Kindled Rats under Conditions of Experimental Epilepsy.” *Molecular Brain Research* 83 (1–2): 44–51. https://doi.org/10.1016/S0169-

328X(00)00195-9.

Squire, Larry, Darwin Berg, Floyd E. Bloom, Sascha du Lac, Anirvan Ghosh, and Nicholas C. Spitzer, eds. 2012. *Fundamental Neuroscience, 4th Edition*. https://www.elsevier.com/books/fundamental-neuroscience/squire/978-0-12-385870-2.

Szyndler, Janusz, Piotr Maciejak, Danuta Turzyńska, Alicja Sobolewska, Ewa Taracha, Anna Skórzewska, Małgorzata Lehner, et al. 2009. "Mapping of C-Fos Expression in the Rat Brain during the Evolution of Pentylenetetrazol-Kindled Seizures." *Epilepsy and Behavior* 16 (2): 216–24. https://doi.org/10.1016/j.yebeh.2009.07.030.

Tamagnini, Francesco, Sarah Scullion, Jonathan T. Brown, and Andrew D. Randall. 2014. "Low Concentrations of the Solvent Dimethyl Sulphoxide Alter Intrinsic Excitability Properties of Cortical and Hippocampal Pyramidal Cells." Edited by Vadim E. Degtyar. *PLoS ONE* 9 (3): e92557. https://doi.org/10.1371/journal.pone.0092557.

Telkes, Ildikó, Péter Kóbor, József Orbán, Tamás Kovács-Öller, Béla Völgyi, and Péter Buzás. 2019. "Connexin-36 Distribution and Layer-Specific Topography in the Cat Retina." *Brain Structure and Function* 224 (6): 2183–97. https://doi.org/10.1007/s00429-019-01876-y.

Téllez-Zenteno, Jose F., and Lizbeth Hernández-Ronquillo. 2012. "A Review of the Epidemiology of Temporal Lobe Epilepsy." *Epilepsy Research and Treatment* 2012: 1–5. https://doi.org/10.1155/2012/630853.

"Types of Epilepsy & Seizure Disorders in Adults | NYU Langone Health." n.d. Accessed August 11, 2020. https://nyulangone.org/conditions/epilepsy-seizure-disorders-in-adults/types.

"Types of Seizures | Epilepsy | CDC." n.d. Accessed August 11, 2020. https://www.cdc.gov/epilepsy/about/types-of-seizures.htm.

Vervaeke, Koen, Andrea LÖrincz, Padraig Gleeson, Matteo Farinella, Zoltan Nusser, and R. Angus Silver. 2010. "Rapid Desynchronization of an Electrically Coupled Interneuron Network with Sparse Excitatory Synaptic Input." *Neuron* 67 (3): 435–51. https://doi.org/10.1016/j.neuron.2010.06.028.

Vincze, Renáta, Márton Péter, Zsolt Szabó, Julianna Kardos, László Héja, and Zsolt Kovács. 2019. "Connexin 43 Differentially Regulates Epileptiform Activity in Models of Convulsive and Non-Convulsive Epilepsies." *Frontiers in Cellular Neuroscience* 13 (April). https://doi.org/10.3389/fncel.2019.00173.

Voss, Logan J, Noortje Mutsaerts, and James W Sleigh. 2010a. "Connexin36 Gap Junction Blockade Is Ineffective at Reducing Seizure-like Event Activity in Neocortical Mouse Slices." *Epilepsy Research and Treatment* 2010 (January): 310753. https://doi.org/10.1155/2010/310753.

———. 2010b. "Connexin36 Gap Junction Blockade Is Ineffective at Reducing Seizure-like Event Activity in Neocortical Mouse Slices." *Epilepsy Research and Treatment* 2010 (January): 310753. https://doi.org/10.1155/2010/310753.

Wang, Yongfu, and Andrei B. Belousov. 2011. "Deletion of Neuronal Gap Junction Protein Connexin 36 Impairs Hippocampal LTP." *Neuroscience Letters* 502 (1): 30–32. https://doi.org/10.1016/j.neulet.2011.07.018.

Wilson, Catherine A., Samantha K. High, Braedan M. McCluskey, Angel Amores, Yi Lin Yan, Tom A. Titus, Jennifer L. Anderson, et al. 2014. "Wild Sex in Zebrafish: Loss of the

Natural Sex Determinant in Domesticated Strains." *Genetics* 198 (3): 1291–1308. https://doi.org/10.1534/genetics.114.169284.

Wu, X.L., D.M. Ma, W. Zhang, J.S. zhou, Y.W. Huo, M. Lu, and F.R. Tang. 2018. "Cx36 in the Mouse Hippocampus during and after Pilocarpine-Induced Status Epilepticus." *Epilepsy Research* 141 (March): 64–72. https://doi.org/10.1016/J.EPLEPSYRES.2018.02.007.

Wu, Xue-mei, Guang-liang Wang, Xiao-sheng Hao, and Jia-chun Feng. 2017. "Dynamic Expression of CX36 Protein in Kainic Acid Kindling Induced Epilepsy." *Translational Neuroscience* 8 (1): 31–36. https://doi.org/10.1515/tnsci-2017-0007.

Wu, Yvonne W, Joseph Sullivan, Sharon S McDaniel, Miriam H Meisler, Eileen M Walsh, Sherian Xu Li, and Michael W Kuzniewicz. 2015. "Incidence of Dravet Syndrome in a US Population." *Pediatrics* 136 (5): e1310-5. https://doi.org/10.1542/peds.2015-1807.

Yang, Huajun, Wei Shan, Fei Zhu, Tingting Yu, Jingjing Fan, Anchen Guo, Fei Li, Xiaofeng Yang, and Qun Wang. 2019. "C-Fos Mapping and EEG Characteristics of Multiple Mice Brain Regions in Pentylenetetrazol-Induced Seizure Mice Model." *Neurological Research* 41 (8): 749–61. https://doi.org/10.1080/01616412.2019.1610839.

Yao, Cong, Kimberly G Vanderpool, Matthew Delfiner, Vanessa Eddy, Alexander G Lucaci, Carolina Soto-Riveros, Thomas Yasumura, John E Rash, and Alberto E Pereda. 2014. "Electrical Synaptic Transmission in Developing Zebrafish: Properties and Molecular Composition of Gap Junctions at a Central Auditory Synapse." *Journal of Neurophysiology* 112 (9): 2102–13. https://doi.org/10.1152/jn.00397.2014.

Yin, Linlin, Lisette A. Maddison, Mingyu Li, Nergis Kara, Matthew C. Lafave, Gaurav K. Varshney, Shawn M. Burgess, James G. Patton, and Wenbiao Chen. 2015. "Multiplex

Conditional Mutagenesis Using Transgenic Expression of Cas9 and SgRNAs." *Genetics* 200 (2): 431–41. https://doi.org/10.1534/genetics.115.176917.

Zack, Matthew M, and Rosemarie Kobau. 2017. "National and State Estimates of the Numbers of Adults and Children with Active Epilepsy - United States, 2015." *MMWR. Morbidity and Mortality Weekly Report* 66 (31): 821–25. https://doi.org/10.15585/mmwr.mm6631a1.